Environmental Science and Pollution Research (2022) 29:10871–10893
https://doi.org/10.1007/s11356-021-17933-1

REVIEW ARTICLE

State-of-the-art biosynthesis of tin oxide nanoparticles by chemical precipitation method towards photocatalytic application

Sumaya Tarannum Nipa[1] · Rumana Akter[1] · Al Raihan[1,2] · Shahriar bin Rasul[1] · Uday Som[1] · Shafi Ahmed[3] · Jahangir Alam[1] · Maksudur Rahman Khan[4] · Stefano Enzo[5] · Wasikur Rahman[1]

Received: 27 July 2021 / Accepted: 30 November 2021 / Published online: 8 January 2022

Abstract

Tin oxide (SnO_2) with versatile properties is of substantial standing for practical application, and improved features of the material are demonstrated in the current issue through the integration of nanotechnology with bio-resources leading to what is termed as biosynthesis of SnO_2 nanoparticles (NPs). This review reveals the recent advances in biosynthesis of SnO_2 NPs by chemical precipitation method focused on distinct methodologies, characterization, and reaction mechanism along with a photocatalytic application for dye degradation. According to available literature reviews, numerous bio-based precursors selectively extracted from biological substrates have effectively been applied as capping or reducing agents to achieve the metal oxide NPs. The major precursor obtained from the aqueous extract of root barks of *Catunaregam spinosa* is found to be *7-hydroxy-6-methoxy-2H-chromen-2-one* that has been proposed as a model compound for the reduction of metal ions into nanoparticles due to having highly active functional groups, being abundant in plants (67.475 wt%), easy to extract, and eco benign. In addition, the photocatalytic activity of SnO_2 NPs for the degradation of organic dyes, pharmaceuticals, and agricultural contaminants has been discussed in the context of a promising bio-reduction mechanism of the synthesis. The final properties are supposed to depend exclusively upon a number of factors, e.g., particle size (< 50 nm), bandgap (< 3.6 eV), crystal defects, and catalysts dosage. With this contribution, it has been perceived not only to provide an overview of recent advances in the biosynthesis of SnO_2 NPs but also to indicate the main issues in need aiming to show vision towards innovative outcomes.

Keywords Nanoparticles · SnO_2 · Biosynthesis · Precipitation method · Reaction mechanism · Application

Introduction

Nanoparticles (NPs) have attracted huge interest from both fundamental science and technological standpoints because their properties exhibit very dramatic differences from higher dimensional counterparts. NPs have immense application in the fields of catalysis, solar cells, sensors, water treatment, and energy storage due to their excellent physical, chemical, electrical, magnetic, optical, and surface properties (Balzani, 2005; Tiwari et al., 2012). Recently, semiconductor NPs have exhibited a broad range of applications in photocatalysis (Chen et al., 2014; Suthakaran et al., 2020), optoelectronics (Nabi et al., 2003), and solar energy conversion (Chappel and Zaban, 2002), owing to their extraordinary features.

Nanostructured materials are single-phase or multiphase polycrystalline solids and are generally characterized by their size, shape, surface area, and disparity (Shahverdi

Responsible Editor: Santiago V. Luis

✉ Wasikur Rahman
w.rahman@just.edu.bd; mwrahman.ump@gmail.com

[1] Department of Chemical Engineering, Jashore University of Science and Technology, Jashore 7408, Bangladesh

[2] Department of Chemistry, University of New Brunswick, Fredericton, New Brunswick E3B 5A3, Canada

[3] Department of Agro Product Processing Technology, Jashore University of Science and Technology, Jashore 7408, Bangladesh

[4] Department of Chemical Engineering, College of Engineering, Universiti Malaysia Pahang, 26300 Pahang, Gambang, Malaysia

[5] Dipartimento Di Chimica E Farmacia, Università Di Sassari, via Vienna n. 2, 07100 Sassari, Italy

et al., 2011). The surface area (i.e., surface-to-mass ratio) of nanometric particles is a thousand times higher than that in micrometric levels (Savolainen et al., 2013). Nanoparticles are technologically advanced in improved strength, chemical reactivity, and conductivity associated with attractive research materials, e.g., carbon nanotubes, metal particles, and polymer composites, devoid of nanoscale features of different shapes and sizes (Fig. 1) (Scott, 2005). Various metal oxide NPs (2–100 nm) are characterized by mostly electromagnetic radiation in the UV/visible range.

Tin oxide NPs typically show striking physical and electrical properties and optical transparency in the visible region (300–800 nm) (Finn et al., 2015). SnO_2 NPs are of particular interest for a variety of applications such as gas sensors (Kennedy et al., 2002); catalysts (Jeong et al., 2014); anodes in lithium batteries (Chandra Bose et al., 2002); raw materials for transparent films, infra-red mirrors, or optoelectronic devices (Mohan et al., 2015); and improved fuel-cells (Guo, 2011). Further studies showed state-of-the-art catalytic performance of SnO_2 NPs with small diameter (~ 2 nm) deposited on a polycrystalline metallic electrode en route for oxidation of methanol or ethanol (Magee et al., 2014). SnO_2 NPs are competent to adsorb water molecules after dissociation results in easier production of CO_2 from total oxidation of ethanol (Li et al., 2013). The reasons behind huge applications of SnO_2 NPs are small particle size as well as the large-specific surface area being essential for high catalytic performances (Zhang and Liu, 1999).

Photocatalytic application of NPs is of current attention in dye degradation because dyes are major toxic chemicals that create environmental pollution (Kostedt et al., 2008; Safavi and Momeni, 2012; Zhang et al., 2009a, 2009b) through discharging effluents and solid wastes all over the world from textiles, cosmetics, foods, drug, and paper industries (Nipa et al., 2019). Complex structures of these dyes are thermodynamically more stable results in difficulties to degrade or eliminate from the effluents. Many physical, chemical, and biological methods were successfully practiced to remove these dyes (Mascolo et al., 2007; Wang et al., 2010a, 2010b). Nanoparticles are stimulated by UV/visible irradiation that generates a redox environment in the system during catalytic degradation (Fatima et al., 2019; Beydoun et al., 1999). In particular, SnO_2 NPs show strong photocatalytic activity towards different dyes under many radiation sources reported elsewhere (Bhattacharjee and Ahmaruzzaman, 2015b; Haritha et al., 2016; Tammina and Mandal, 2016). As photodegradation reaction is influenced by photocatalysts (Ajoudanian and Nezamzadeh–Ejhieh, 2015; Derikvandi and Nezamzadeh–Ejhieh, 2017; Ahmad et al., 2016), new strategies are currently demanded to synthesize different nanoparticles with desired properties.

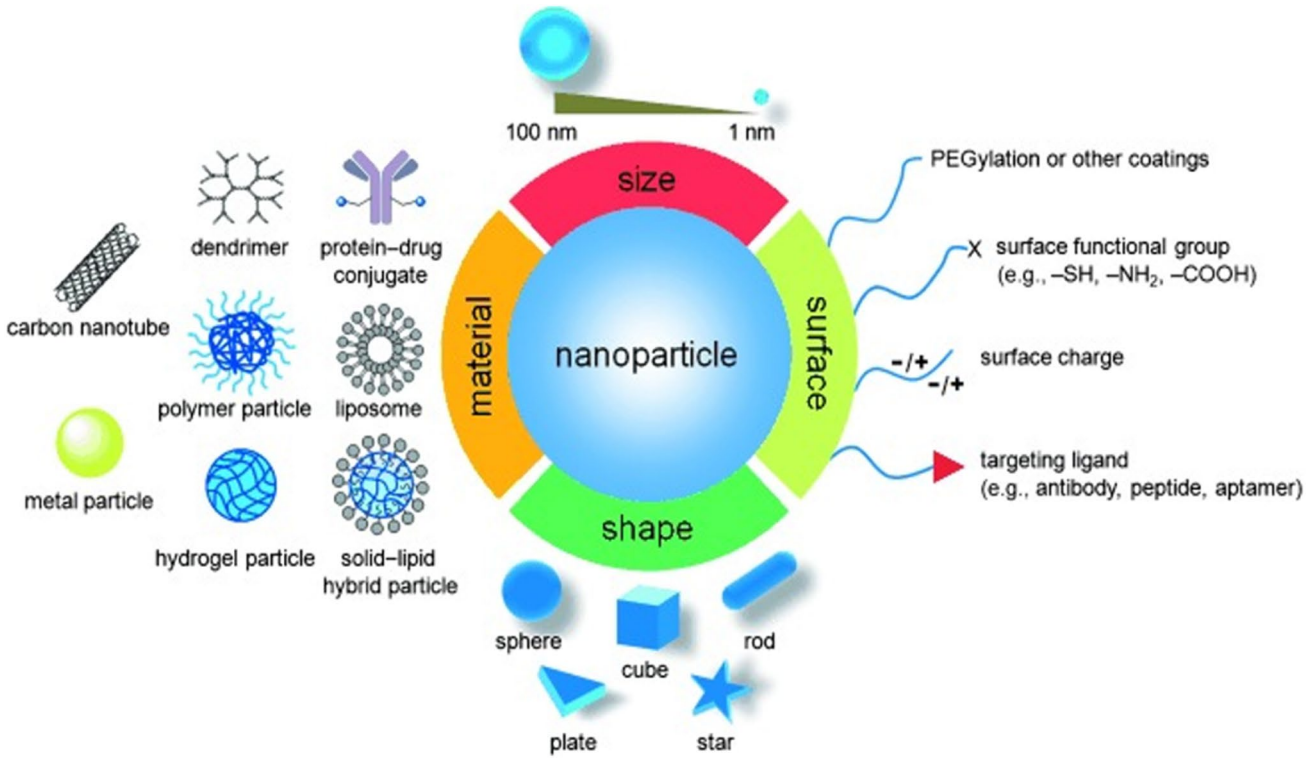

Fig. 1 Properties of nanoparticles

Varied physical and chemical methods are generally employed for synthesizing and fabricating nanostructured materials (Ong et al., 2018). The methods for preparing NPs usually involve either a "top-down" or a "bottom-up" approach (Fig. 2). Size reduction of suitable macro-molecules is starting material for the top-down method; whereas, the bottom-up points out the fabrication of particles from micro-entities. The top-down method suffers drawbacks from surface imperfection structures of the NPs (Thakkar et al., 2010), and the bottom-up mostly counts on chemico–biological methods, where nanostructured building blocks are initially formed and then assembled to obtain the preferred products.

Synthetic methods of SnO_2 NPs, in particular, have been developed in the last few years based on peroxide (Hoffmann et al., 1995) and polymeric precursors (Fu et al., 2011; Yang et al., 2011) such as hydrothermal (Chu et al., 2014), sol–gel (Wang et al., 2015), co-precipitation (Agrahari et al., 2015), microemulsion (Zamand et al., 2014), and chemical precipitation methods (Bhattacharjee et al., 2015) because of their wide range of applications. Temperature is an obviously important factor for the heat treatment method as the precursors are processed at different temperatures and time intervals to achieve materials with a single crystalline phase (Stanulis et al., 2012). Solid-state reactions are the basis of SnO_2 synthesis over the peroxide precursor method (Guo et al., 2016). Polymeric precursor–based techniques, in general, are complying with an esterification reaction between metallic citrate and ethylene glycol through chelation of metallic cation designed for polymeric chain formation (Lei et al., 2007).

Among these strategies, the chemical precipitation method is particularly attractive thanks to its fast production period, clean phases, amazing crystal structure formation, and being cost-effective. The synthesis of innovative materials is combined with versatility in process design that offers good chemical homogeneity due to proper mixing at the molecular level (Das, 2001). SnO_2 NPs can be prepared by the method using either chemical reagents (Cocco et al., 1987; Kawashima et al., 2012; Naje, 2003) or green biological precursors known as biosynthesis (Elango et al., 2015; Gaber et al., 2013; Viju Kumar and Prem, 2018). Biosynthesis uses biological substrates obtained from the extracts of plants, bacteria, fungus, and algae to substitute commercially

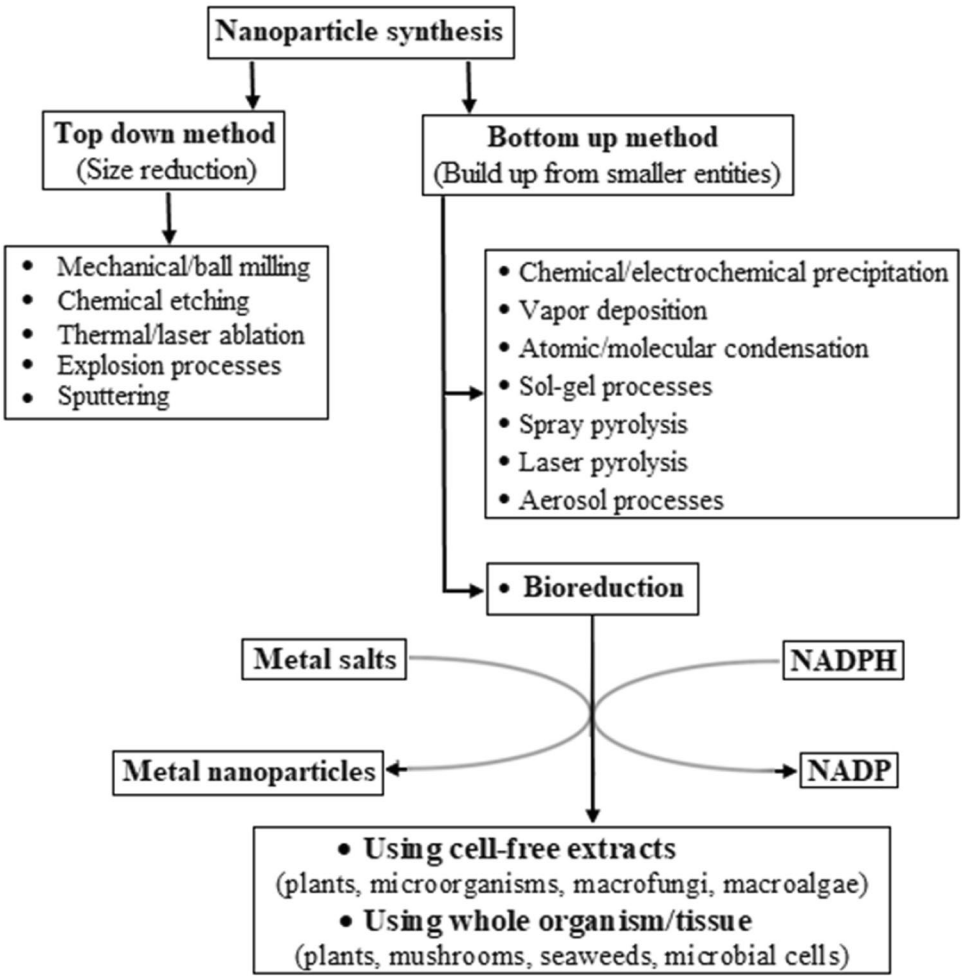

Fig. 2 Various methods for preparing nanoparticles (Madkour, 2017)

available chemical solvents and stabilizers to reduce toxic properties of the process (Kharissova et al., 2013; Król et al., 2017). In the case of SnO_2 NPs synthesis, numerous bio-based precursors selectively extracted from biological substrates have effectively been applied as capping or reducing agents to achieve metal oxide NPs. Recently, Matussin et al. (2020) reported green biosynthesis of SnO_2 NPs using various plant extracts and demonstrated their effects on the optical and structural properties of the as-prepared SnO_2 NPs with possible applications in practical arenas (Matussin et al., 2020). In general, the biosynthesis of SnO_2 NPs is a very straightforward process in which tin salts are added to a biological extract for bio-reduction or complex formation, followed by the proper centrifugation and thermal treatment of the precipitate after the reaction, and finally, SnO_2 nanopowder is obtained (Celina Selvakumari et al., 2018; Haritha et al., 2016). In fact, the particle size of dispersed phases is a function of temperature, pH, and degree of distribution (Lq et al., n.d.). Elevated temperatures, in contrast, are needed to obtain outstanding crystalline SnO_2 NPs with the drawback of the high degree of aggregation during successive drying and calcination processes.

Even though an extensive quantity of research outcomes have been reported in this field, however, there is no comprehensive review article based on the biosynthesis of SnO_2 NPs by mostly using the chemical precipitation method. In addition, the reaction mechanism of the nanoparticle formation and photocatalytic degradation of dyes have still to be defined and understood due to the high complexity of the biological extracts besides thermodynamically stable structures of dyes. From this viewpoint, the review summarizes recent advances in the synthetic methods of SnO_2 NPs; in particular, the chemical precipitation method focused on distinct methodologies applied, characterization, and bio-reduction mechanism of the synthesis with different biological substrates along with the photocatalytic application for dye degradation.

Properties of SnO_2 NPs

Semiconductor metal oxide nanoparticles, predominantly SnO_2 NPs with rutile structure, play a vital role in the conversion of metal ions into nanoparticles, photocatalytic degradation of textile dyes, reduction of heavy metals, etc. because of higher surface area, less toxic effect, more thermal conductivity, and sensitivity (Cao et al., 2006; Kawashima et al., 2012). SnO_2 is an amphoteric white- or gray-colored solid that represents high optical transparency and reflectivity in the region of IR radiation. It is one of the n-type (oxygen-deficient) semiconductor materials with a wide bandgap (3.6 eV). Oxygen vacancies are responsible for n-type behavior that corresponds to photoactivation in the UV range of 350 nm, making this material an ideal photocatalyst for the degradation of a variety of organic pollutants and has large excitation binding energy (130 meV) (Liu et al., 2010). Moreover, it works as a chemical sensor that instigates a decrease in the surface barrier properties and leads to a change in conductance through oxidation reaction between chemical species and chemisorbed oxygen (Kar and Patra, 2014). Some physical and crystallographic properties of SnO_2 NPs are shown in Table 1 (Houari et al., 2014).

SnO_2 NPs are available in the form of faceted high surface area diamagnetic oxide nanostructures. Nanoscale SnO_2 is typically 20–40 nm with a specific surface area in the range of 10–80 m^2g^{-1} and is also available in rutile, ultra-high purity, transparent, coated, and dispersed forms.

Tin element is practiced with mostly three oxidation states (+2, +3, and +4); therefore, it forms three oxides, e.g., SnO, Sn_2O_3, and SnO_2, known as amphoteric oxide of tin, and three Sn states exist in the oxide films that can be labeled as metallic, quasimetallic, and oxidic Sn. The quasimetallic Sn is an intermediate state resulting from oxidized Sn and is still alloyed within other metal surface layers. Tin(II) oxide (SnO, stannous oxide) is a stable blue–black and metastable red form. Tin(IV) oxide (SnO_2, stannic oxide) is called cassiterite, and it is the main ore of tin. When SnO is heated in an inert atmosphere, initially disproportionation reaction occurs, producing Sn_3O_4 that further reacts to generate SnO_2 (Wiberg, 2002). In fact, SnO is a thermodynamically unstable phase that leads to the formation of the more stable tetragonal rutile-type SnO_2 structure and β-Sn over relatively high temperatures (Cusack, 1998; Giefers et al., 2005; Krishnakumar et al., 2008; Moreno et al., 2001).

The standing of metal substrates in striking structure and crystallographic orientation on oxide films is demonstrated by spectrometric analysis. To evaluate the purity of SnO_2 NPs in the form of powder samples, crystal structure and crystallinity are assessed by X-ray diffraction (XRD) analysis (Rahman et al., 2011). Mevada et al. (2020) reported the XRD pattern of commercial SnO_2 NPs (Sigma

Table 1 Selected physical and crystallographic properties of SnO_2 NPs (Houari et al., 2014)

Element (wt%)	Sn: 78.76 and O: 21.21
Molecular weight (g/mol)	150.69
Density (g/cm^3)	6.90
Melting point (℃)	1500–1630
Boiling point (℃)	1800–1900
Crystal system	Tetragonal
Space group	$P4_2/mnm$
Lattice constant (nm)	a = b = 0.47374 and c = 0.31864
Electronic configuration	Sn: [Kr] $4d^{10}$ $5s^2$ $5p^2$ O: [He] $2s^2$ $2p^4$

Aldrich Chemie GmbH, Steinheim, Germany) shown in Fig. 3 (Mevada et al., 2020). The diffraction peaks for the SnO_2 NPs obtained at 26.20°, 33.9°, 37.96°, 51.80°, 54.78°, 57.80°, 61.90°, 64.74°, 65.98°, 71.32°, and 78.74° corresponding to the planes (110), (101), (200), (211), (220), (002), (310), (112), (301), (202), and (321) (Fig. 3a). It is well known that the sensing features of SnO_2 are dominantly controlled by surface properties. In particular, the (110) plane is one of the most thermodynamically stable surfaces among the indexed surfaces (Oviedo and Gillan, 2002, 2001; Wang et al., 2008; Zhang et al., 2011), and it has widely been used to investigate the surface characteristics of SnO_2 (Batzill et al., 2003). SnO_2 NPs of the tetragonal crystal system with rutile structure were confirmed by the observed peak positions (Batzill et al., 2004; Celina Selvakumari et al., 2018; Letia and Groza, 2009) and compared with standard Bragg positions (Fig. 3a) point out a good agreement with standard database (JCPDS 41–1445) (Begum et al., 2016; Patil et al., 2012). The packing diagram of SnO_2 NPs is shown in Fig. 3b (Veerabhadrayya et al., 2018).

SnO_2 has space group $P4_2/mnm$, and symmetries of optical modes ($k=0$), including IR and Raman, are D_{4h}. Its unit cell crystallizes to rutile structure where each Sn atom (blue) is coordinated by six O atoms (red), i.e., the coordination number of Sn 6; whereas, each O atom is coordinated by three Sn atoms, i.e., the coordination number of O_3 (Fig. 3b) (Batzill et al., 2004; Chen et al., 2012; Greenwood and Earnshaw (n.d.); Veerabhadrayya et al., 2018). The octahedral structure of SnO_2 shares the edges and forms a linear chain along the *c*-axis, where maximum electron density and high polarization are observed (Celina Selvakumari et al., 2018).

In addition, the crystallite size of nanomaterials is usually calculated by Scherrer's equation, and the average size of SnO_2 NPs was found to be ~ 20 nm for a stronger peak at (110) reported elsewhere (Bhattacharjee et al., 2015, 2014; Bhattacharjee and Ahmaruzzaman, 2015a). The particle size and strain, annealing temperature, and orientation of crystals affect the height and shape of the diffraction peaks across various planes of Miller indices (hkl), as revealed from the XRD patterns (Mevada et al., 2020).

TEM analysis is typically employed to identify the morphology, size, d-spacing, and crystalline nature of SnO_2 NPs. Figure 4 shows TEM, particle size distribution, HR-TEM, and SAED pattern of the photocatalyst. The spherical shape of SnO_2 NPs with an average radius of 2–3 nm was detected by the TEM image (Fig. 4a) (Bakrania and Wooldridge,

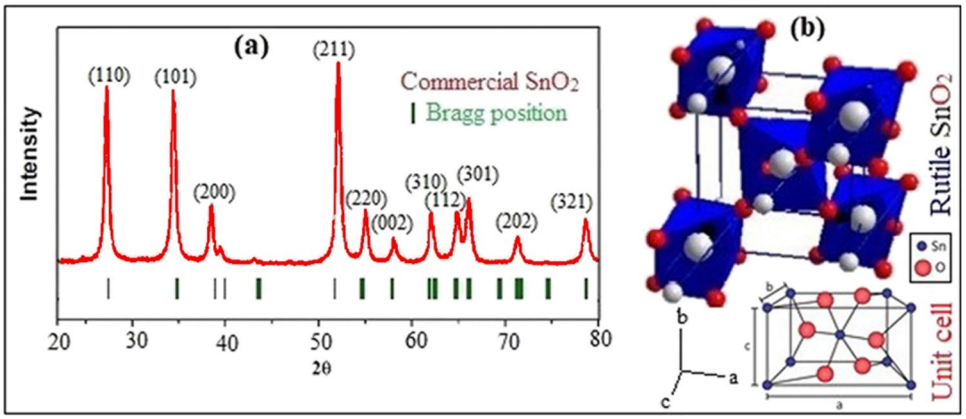

Fig. 3 (**a**) XRD pattern of commercial SnO_2 ; **modified** from Mevada et al. (2020) and (**b**) Packing diagram of tetragonal crystal system of SnO_2 NPs with a unit cell of rutile SnO_2 (below) (Batzill et al., 2004 **Veerabhadrayya** et al., 2018)

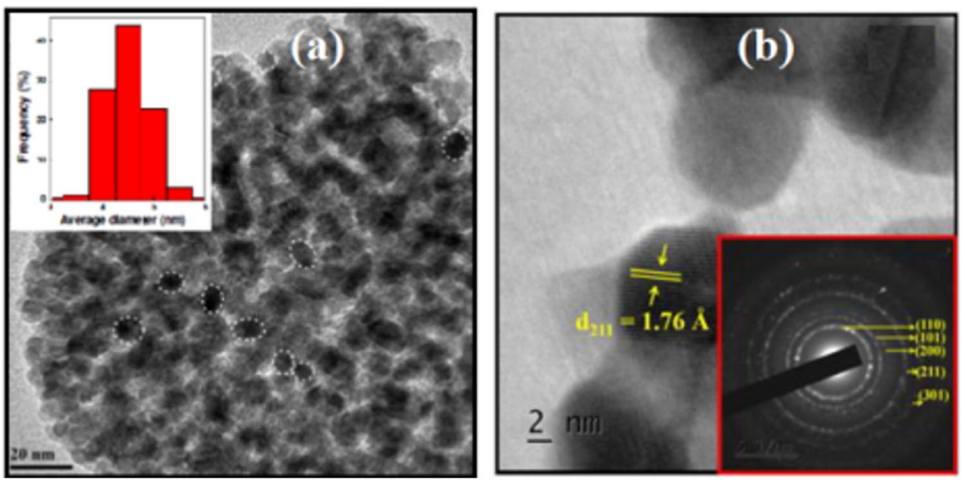

Fig. 4 (**a**) TEM image of SnO_2 NPs with 20 nm magnification and histogram (inset) showing the particle size distribution; (**b**) HR-TEM for d-spacing and SAED pattern (inset) (Bhattacharjee and Ahmaruzzaman, 2015c; Celina Selvakumari et al., 2018; Thakkar et al., 2010)

2009). Size distribution of SnO_2 NPs is represented by a histogram shown in Fig. 4a (inset), resulting in a mean particle radius of 2.25 nm (Bhattacharjee and Ahmaruzzaman, 2015b).

HR-TEM image of SnO_2 NPs clearly demonstrates lattice fringes of the nanomaterials, and inter-planar spacing obtained is $d_{211} = 1.76$ Å that corresponds to lattice plane (211) (Fig. 4b). The crystalline nature of SnO_2 NPs is perceived in the SAED pattern (Fig. 4b, inset), and the lattice spacing was calculated corresponding to (110), (101), (211), and (301) planes (Celina Selvakumari et al., 2018). The bright field with multiple rings denoted in the SAED pattern revealed polycrystallinity of SnO_2 NPs, and Miller indices (hkl) values of the rings verified the rutile crystal structure of the nanoparticles (Bhattacharjee et al., 2014; Bhattacharjee and Ahmaruzzaman, 2015b; Celina Selvakumari et al., 2018).

Moreover, it can be exposed from the TEM analysis that particle size is influenced by the annealing temperature of the precursor materials towards SnO_2 NPs synthesis. The crystallinity of the NPs increases with increasing temperature thru reducing the defects owing to the systematic arrangement of the atoms in the unit cell that leads to a rise in particle size. It is interesting to be mentioned that SnO_2 NPs can be synthesized with desired size monitoring calcination temperature (Babar et al., 2010; Celina Selvakumari et al., 2018; Tammina et al., 2018). In a nutshell, the electron microscopic results point out that the particle size and lattice plane of the nanoparticles are in well agreement with XRD.

Classification of SnO_2 NPs

Diverse nanostructures of SnO_2 viz., namely nanocrystals, nanowires, nanotubes, nanodots, and nanobelts, are technologically important due to their size-dependent properties. Additional nanostructures include nanorods, nanohorns, nanowhiskers, nanopyramides, and nanocomposites. The particles are preferentially adsorbed at the surface interface using chemically bound polymeric materials on account of surface-functionalized properties (Nilavazhagan et al., 2014).

Based on dimensions, SnO_2 can be divided into one-dimensional (1D), two-dimensional (2D), and three-dimensional (3D) nanostructures. They exhibit novel physicochemical characteristics that considerably differ from conventional bulk materials (Park et al., 2007). Figure 5 shows the morphologies of tin oxides having different dimensions. 1D nanostructures have an intense impact on nanoelectronics, nanocomposites, nanodevices, energy resources, and national security (Zhang et al., 2012). 2D structures are exclusively interesting, owing to understanding the basic mechanism of nanoparticle growth besides investigation and application in nanosensors and photocatalysis (Zeng

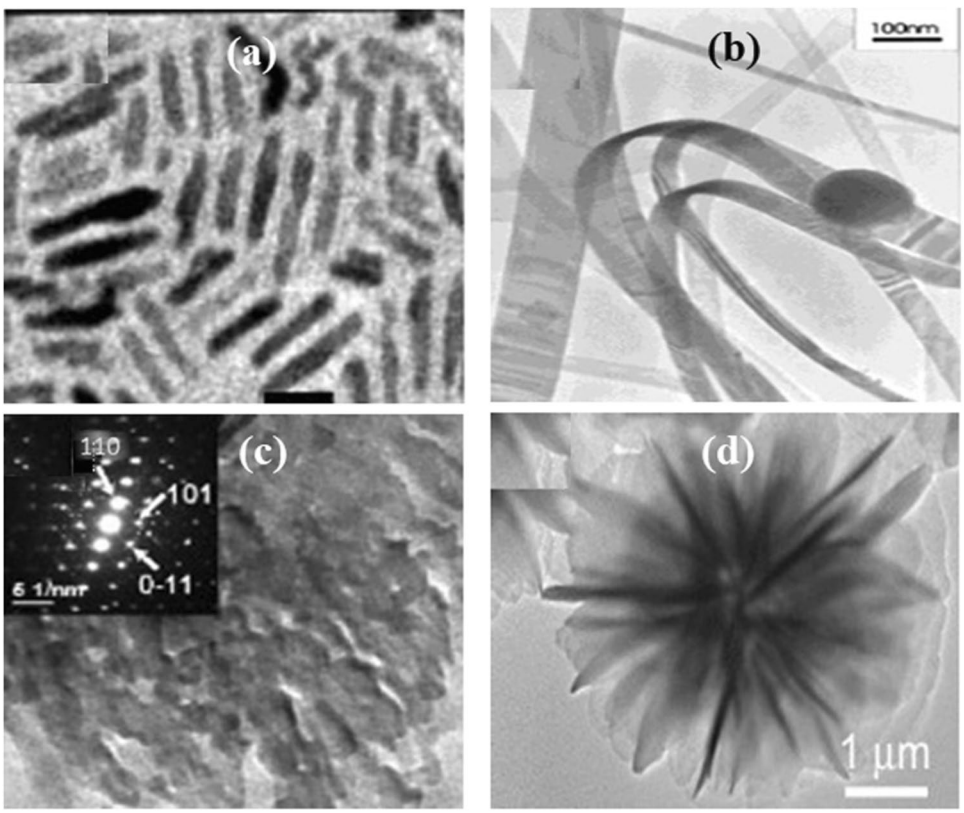

Fig. 5 TEM images of different nanostructured SnO_2 NPs: (**A**) 1D nanorods, (**B**) 1D nanoribbons, (**C**) 2D nanosheets, and (**D**) 3D-nanostructures (Cheng et al., 2004; Hu et al., 2002; Wu et al., 2011; Zhong et al., 2006)

et al., 2009). In addition, 3D nanostructures are frequently employed as catalysts, magnetic materials, and electrodes for batteries (Kim, 2014). In general, 1D includes nanorods (Park et al., 2007), nanowires (Meduri et al., 2009), nanoribbon (Dai et al., 2001), and nanotubes (Dai et al., 2002); whereas, 2D consists of nanosheets, branched structures, nanoprisms, nanoplates, nanowalls, and nanodisks (Parwaz Khan et al., 2016), and 3D comprises flower-type hollow or porous nanostructures (Wang et al., 2010a, 2010b). It can be pointed out that nanostructure materials with low-dimensional, for instance, 1D or 2D, are more competent to withstand volume change during the charge–discharge process (Wang et al., 2010a, 2010b). Momeni et al. (2016a, 2016b) used the atomistic simulation method to reveal the intrinsic structural change of SnO_2 that brings down dimensions from 2D nanosheets to 1D nanorods of monolayer materials (Momeni et al., 2016a, 2016b). It is attractive for having a higher surface-area-to-volume ratio and supplies adequate absorption molecules aimed at various nanostructures (1D, 2D, and 3D) involved in a small space (Jung et al., 2008; Chang et al., 2020).

Biosynthesis of SnO_2 NPs

Various physical and chemical methods are, in general, employed to synthesize and fabricate nanostructured materials (Haritha et al., 2016). Researchers are currently exploring biosynthetic methods to improve the production of metal and metal oxide NPs using clean technologies rather than chemical and physical methods commonly used in industry (Kharissova et al., 2013; Król et al., 2017; Muthuvinothini and Stella, 2019; Shah et al., 2015; Zikalala et al., 2018). Recently, the biosynthesis of SnO_2 NPs has gained huge attention for its various important applications. Nevertheless, commercially available SnO_2 are considered much expensive due to costly precursor materials, difficulties in synthetic technique, complications in separation, etc. This has led to a growing research interest in the production of SnO_2 NPs from bio-resources, renewable, widely available, nontoxic, and cost-effective precursors. The chemical precipitation method is now considered as one of the best available processes for the synthesis of SnO_2 NPs. The NPs can be synthesized either by using chemical reagents (Cocco et al., 1987; Kawashima et al., 2012; Naje, 2003) or from green biological precursors (Elango et al., 2015; Gaber et al., 2013; Viju Kumar and Prem, 2018); whether the later one is predominant and will be discussed in the current issue.

Reaction procedures

Haritha et al. (2016) showed the green chemical production of SnO_2 NPs using $SnCl_2$ solution mixed with *Catunaregam spinosa* aqueous extract and placed in a water bath at 60℃ for 2 h. Then, the mixture was centrifuged, followed by washing and heating at 450℃ for 2 h to get the NPs (Haritha et al., 2016). A biological method was discussed by Hong et al. (2017). The group placed $SnCl_2$ solution in an incubator, and aqueous extract of the *Litsea cubeba* fruit was added at room temperature with an agitation of 100 rpm for 10 min. Then, the precipitate was centrifuged in turn washing and drying at 50℃ for 2 h (Hong and Jiang, 2017). Elango et al. (2015) reported an additional biological method using an almost similar procedure. In this case, methanolic extract of *P. americana* seed was mixed with $SnCl_2.2H_2O$ at 60℃ for 12 h (Elango et al., 2015). Merlin et al. (2018) proposed a simple method using *Stevia rebaudiana* extract. Ethanolic extract of *S. rebaudiana* was mixed with SnO_2 aqueous solution and heated at 80℃ (Viju Kumar and Prem, 2018). Bhattacharjee et al. (2015) showed the synthesis method by using amino acid and arginine. $SnCl_2.2H_2O$ was treated with an equimolar aqueous solution of arginine and irradiated with 300 W shots in a microwave oven (Bhattacharjee and Ahmaruzzaman, 2015c). Tammina and Mandal (2016) exposed the use of amino acid and tyrosine to synthesize SnO_2 NPs. $SnCl_2.2H_2O$ was added with tyrosine solution and stirred at 100℃ for 4 h (Tammina and Mandal, 2016). Gaber et al. (2013) presented the conventional precipitation method by using an ammonia solution. $NH_3.H_2O$ (30%) was added with $SnCl_4.5H_2O$ dropwise to control pH 8 at 40℃. After that, it was centrifuged at 3000 rpm for 20 min and obtained white gel precipitation, followed by annealing at a temperature in the range of 300–1050℃ for 2 h (Gaber et al., 2013). Similar methods are also reported elsewhere (Drzymała et al., 2017). Santhi et al. (2016) explored the method of dissolving $SnCl_2.2H_2O$ in NaOH, and HCl was added dropwise up to pH 5 (Santhi et al., 2016). Another method was studied by Ibarguen et al. (2007) using ammonium hydroxide and diethylamine (Ibarguen et al., 2007). Song and Kang (2000) proposed urea instead of ammonia or ammonium hydroxide. Urea (0.1–1.0 M) was dissolved in $SnCl_4.5H_2O$ aqueous solution. Then, it was hydrolyzed at 90℃ for 4 h and cooled down to get the final product. Prior to this, the mixture was successfully centrifuged at high speed (8500 rpm for 30 min), dried in an oven at 100℃ for 24 h, and annealed at 600℃ for 2 h (Song and Kang, 2000). Selvi et al. (2018) used urea along with $Ni(NO_3)_2{\cdot}6H_2O$ for the synthesis of SnO_2 NPs (Thamarai Selvi and Meenakshi Sundar, 2018). Shaikh et al. (2018) used $SnCl_4.5H_2O$, $Sr(NO_3)_2.6H_2O$, and liquor ammonia in defined proportion (Shaikh et al., 2018). Deosarkar et al. (2013) exhibited the use of graphene oxide and $SnCl_2{\cdot}2H_2O$ under ultrasonic irradiation (Deosarkar et al., 2013). Bhattacharjee et al. (2016) showed the utilization of glycerol with stannic chloride by microwave heating method for green synthesis (Bhattacharjee et al., 2016). The

low-temperature situ-precipitation technique was reported by Jia et al. (2014) using $Zn(Ac)_2{\cdot}2H_2O$, $Na_2HPO_4{\cdot}12H_2O$, and $(CH_2)_6N_4$ (Chu et al., 2014). In parallel, Nilavazhagan et al. (2014) used $SnCl_4.5H_2O$ with some other chemicals like $LaCl_3.7H_2O$ and $CuCl_2.2H_2O$, and the method followed the previous procedures (Nilavazhagan et al., 2014). Metal Sn, HCl, HNO_3, and ethanol were used to synthesize SnO_2 NPs by Liang et al. (2017). Firstly, Sn was dissolved in HCl/HNO_3 mixture, and a fixed amount of HNO_3 and ethanol was mixed into it. The solution was then added into deionized water, and pH 3 was controlled at 65℃ by adding polyvinyl alcohol and NH_4OH solution. The precipitate was dried at 100℃ and calcined at 350–600℃ for 2 h after filtration and washing with water and ethanol in succession (Liang et al., 2017). Begum and Ahmaruzzaman (2018) showed an additional chemical precipitation method using surfactant (CTAB), anhydrous aspartic acid with $SnCl_2.2H_2O$ solution following the technique discussed earlier (Begum and Ahmaruzzaman, 2018). From the literature reviews, it can be pointed out that most of the researchers are interested in tin salts (e.g., $SnCl_2.2H_2O$ and $SnCl_4.5H_2O$) as a source of Sn because they are cheap and available worldwide. Of the different capping/reducing agents listed in Table 2, green bio-based chemicals are preferred with reaction conditions, e.g., centrifugation rate 100–5000 rpm at controlled pH, calcination temperature 100–800℃ for ~ 2 h. Table 2 shows varied synthesis methods of SnO_2 NPs, capping/reducing agents, crystal structures, and particle size.

In addition, various characterization methods were used to determine the properties of SnO_2 NPs: FTIR (Cusack, 1998; Moreno et al., 2001), UV/visible spectroscopy (Giefers et al., 2005; Moreno et al., 2001), XRD

Table 2 Synthesis methods of SnO_2 NPs, capping/reducing agents for tin salts reduction, crystal structures, and particle size

Sl. no	Synthesis method	Capping/reducing agent	Crystal structure	Particle size (nm)	Reference
1	Green synthesis by chemical precipitation (ppt)	*Catunaregam spinosa* root bark	Spherical	47 ± 2	Elango et al. (2015)
2	Biological synthesis by chemical ppt	*Litsea cubeba* fruit	Irregular morphology	30	Viju Kumar and Prem (2018)
3	Green synthesis by chemical ppt	*Persia americana* seed	–	4	Tammina and Mandal (2016)
4	Green synthesis by microwave irradiation	Amino acid, arginine	Spherical	4–5	Bhattacharjee and Ahmaruzzaman (2015b)
5	Conventional ppt	Ammonia	Tetragonal	3.45–23.5	Naje (2003)
6	Chemical ppt and microwave irradiation	Ammonia, citric acid, ethylene glycol	Tetragonal	2–10	Santhi et al. (2016)
7	Chemical ppt	Amino acid, tyrosine	Tetragonal, polycrystalline	15–20	Drzymała et al. (2017)
8	In situ chemical ppt	Graphene oxide	–	3–5	Jia et al. (2014)
9	Green synthesis by microwave irradiation	Glycerol	Spherical	8–30	Nilavazhagan et al. (2014)
10	Low-temperature situ ppt	$Zn(Ac)_2{\cdot}2H_2O$, $Na_2HPO_4{\cdot}12H_2O$, $(CH_2)_6N_4$	–	–	Liang et al. (2017)
11	Simple co-ppt	$LaCl_3.7H_2O$, $CuCl_2.2H_2O$, NaOH	Tetragonal rutile	–	Begum and Ahmaruzzaman (2018)
12	Microwave irradiation	NaOH, HCl	Tetragonal	–	Thamarai Selvi and Meenakshi Sundar (2018)
13	Chemical ppt	HCl, HNO_3, ethanol	–	Tunable size	Arularasu et al. (2017)
14	Controlled ppt	NH_4OH	–	< 50	Thamarai Selvi and Meenakshi Sundar (2018)
15	Chemical ppt	Ammonia	Tetragonal rutile	73	Ibarguen et al. (2007)
16	Homogeneous ppt	Urea	–	3–4	Shaikh et al. (2018)
17	Green synthesis	*Stevia rebaudiana*	–	–	Gaber et al. (2013)
18	Microwave-assisted solvothermal	$Ni(NO_3)_2{\cdot}6H_2O$, urea	Tetragonal rutile	10–14	Deosarkar et al. (2013)
19	Co-ppt	Ammonia	Tetragonal	–	Chen et al. (2014)
20	Chemical ppt	Aspartic acid, surfactant (CTAB)	–	8–13.5	Ashour (2018)
21	Chemical synthesis	Ammonia	Tetragonal	14	Chen et al. (2014)
22	Facile co-ppt	Ammonia, $Sr(NO_3)_2.6H_2O$	–	~ 3.7	Bhattacharjee et al. (2016)

(Bhattacharjee and Ahmaruzzaman, 2015b, Bhattacharjee and Ahmaruzzaman, 2015b; Moreno et al., 2001), SEM (Bakrania and Wooldridge, 2009; Krishnakumar et al., 2008), TEM (Bhattacharjee and Ahmaruzzaman, 2015a; Rahman et al., 2011), STEM (Zhang et al., 2011), SPM (Patil et al., 2012), SAED (Bhattacharjee and Ahmaruzzaman, 2015a; Rahman et al., 2011), TGA (Begum et al., 2016; Mevada et al., 2020), DTA (Begum et al., 2016; Mevada et al., 2020), DLS (Oviedo and Gillan, 2001), BET (Greenwood and Earnshaw (n.d.); Patil et al., 2012), DRS (Batzill et al., 2003), XPS (Batzill et al., 2003; Bhattacharjee et al., 2014), PLS (Bhattacharjee et al., 2014; Chen et al., 2012), GC–MS (Moreno et al., 2001), EDX (Bakrania and Wooldridge, 2009; Batzill et al., 2004; Krishnakumar et al., 2008; Moreno et al., 2001; Oviedo and Gillan, 2001; Zhang et al., 2011), VSM (Bhattacharjee and Ahmaruzzaman, 2015d), HR-TEM (Bhattacharjee and Ahmaruzzaman, 2015c; Oviedo and Gillan, 2001), FE-SEM (Batzill et al., 2003; Bhattacharjee and Ahmaruzzaman, 2015b), TG-DSC (Batzill et al., 2004, 2003), UV-DRS (Celina Selvakumari et al., 2018), TEM/EDAX (Moreno et al., 2001), SEM/EDAX (Bhattacharjee and Ahmaruzzaman, 2015c; Giefers et al., 2005), DTA/TGA (N. N. Greenwood, n.d.), etc.

Reaction mechanism

Recently, biosynthesis of nanoparticles has been a more interesting method to reduce metal ions into metal oxide nanoparticles. Bio-based precursors are hydrophilic, biocompatible, nontoxic, and cost-effective in nature and used in diversified fields with exciting morphologies and varied sizes. There are three crucial factors to synthesize and stabilize nanoparticles, i.e., reaction medium, capping, and reducing agents. The reducing agents or complex-forming compounds involved include various water-soluble plant metabolites (e.g., alkaloids, phenolic compounds, terpenoids, flavonoids, saponins, steroids, tannins, and other nutritional compounds), co-enzymes, and bio-waste materials (Batzill et al., 2004). The bio-based resources are comprised of polysaccharides, proteins, and lipids that act as a capping agent that limits the uses of non-biodegradable commercial surfactants. Many researchers showed their interest in the biosynthesis of different metals and metal oxide NPs available in the literature.

Tammina et al. (2018) synthesized SnO_2 NPs of different sizes from $SnCl_2.2H_2O$ and ascorbic acid and reported a plausible mechanism of the redox reaction (Tammina et al., 2018). Haritha et al. (2016) prepared SnO_2 NPs using *C. spinosa* root bark and identified the phytoconstituents of the bark. The major component of the extract (67.475 wt%) was found *7-hydroxy-6-methoxy-2H-chromen-2-one* that can act as an active capping agent for the conversion of Sn^{2+} salts into SnO_2 NPs (Elango et al., 2015). *Sargassum muticum* extract consisted of basic polysaccharides that reduce ferric salts into metal oxide NPs. Protein, as a major component of alga, is responsible for the reduction of nanoparticles and their stabilization (Mevada et al., 2020; Nagarajan and Arumugam Kuppusamy, 2013). The leaf of *Delonix regia* that consisted of gallic acid is responsible for the biosynthesis of palladium NPs (Dauthal and Mukhopadhyay, 2013). Elango et al. (2015) synthesized SnO_2 NPs using the seed of *Persia americana* to have methanolic extract annealed at 300–500℃ and described the phyto-synthesizing property of transition metals, thanks to biocompatibility, low toxicity, eco-friendly, and green phenomena (Elango et al., 2015). Selvakumari et al. (2018) also investigated eggshell membrane (ESM) and pointed out that the key constituents of the membrane are amino acids and aldehydes having functional groups of amino, carboxyl, and carbonyl on the ESM, which acts as a reducing agent, and its properties are comparable to the published results (Celina Selvakumari et al., 2018).

From the discussion, it can be noted that various bio-based capping, reducing, or complexing agents with almost similar properties are accountable for cationic reduction. The hetero-compound *7-hydroxy-6-methoxy-2H-chromen-2-one* obtained from the *C. spinosa* extract has been proposed as a model complex or adduct forming agent for the transformation of metal ions into NPs because it is bio-based, abundant in a plant, easy to extract, and has highly active functional groups. On the other hand, the bio-precursor having aldehyde functional groups can react with tin salts for the reduction of surface-adsorbed Sn^{2+} into Sn^0. Further conversion of Sn^0 into SnO_2 NPs is carried out through atmospheric oxidation. The schematic presentation of the chemical precipitation method for the production of SnO_2 NPs over the reduction of Sn^{2+} salt by reducing agents (e.g., aldehyde, amino acid) is shown in Scheme 1.

According to Scheme 1, stannous ion (Sn^{2+}) is reduced to elemental tin that is precipitated out from the first step of the biosynthesis, where bio-based precursors are used as reducing agents. In fact, the biological substrates having hydrophilic and hydrophobic domains contribute to surface adsorption where the hydrophilic end groups absorb Sn^{2+} ions and hydrophobic parts interact through the formation of H_2 bonding (Celina Selvakumari et al., 2018; Devi et al., 2012). In the second step, the elemental tin (Sn) is oxidized to stannic(IV) oxide (SnO_2) thru calcination in the presence of air. It is noted that the oxidation of elemental tin in an aqueous medium is usually inactive, and it starts to oxidize at a temperature of over 150℃ (Cho et al., 2005), possibly at 232℃ (mp of Sn) or onward temperature settings. The basic reaction of this conversion is as follows:

$$Sn_{(l)} + O_{2(g)} \overset{\Delta}{\Rightarrow} SnO_{2(s)}$$

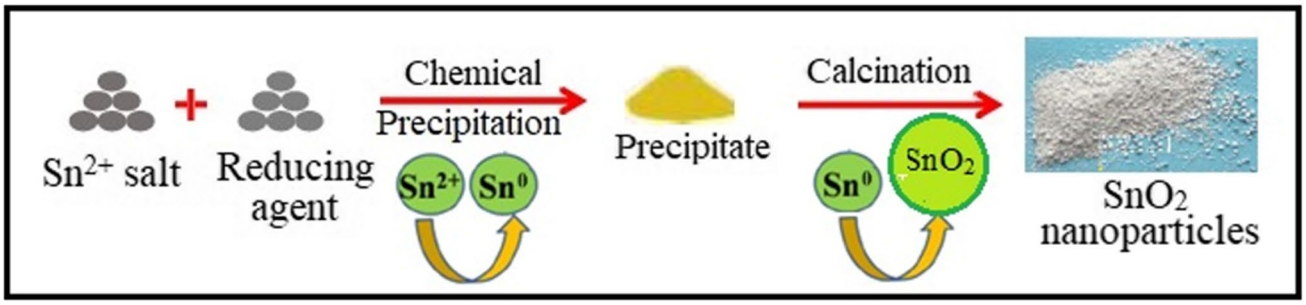

Scheme 1 Schematic presentation of chemical precipitation method for the preparation of SnO_2 NPs by a reducing agent

Celina Selvakumari et al. (2018) also described a mechanism comparable to Scheme 1, where the eggshell membrane was used as a bio-precursor (Celina Selvakumari et al., 2018). It was reported that the aldehyde group shows reducing properties as well as reduced the surface-adsorbed Sn(II) into Sn(0) prior to annealing at 600℃ in natural air to obtain SnO_2 NPs.

The reaction mechanism of SnO_2 synthesis by a reducing agent *7-hydroxy-6-methoxy-2H-chromen-2-one* (HMC) proposed in the context has been illustrated in Scheme 2. The HMC is a water-soluble polar compound being a source of electrons from the chromenone ring and carbonyl double bonds. In addition, the electrons obtained from the lone pair of hydroxyl groups (OH^-) and double bonds take part in the conjugated reaction to form vinyl-based carboxylic compounds prior to the generation of electrons and protons in the system. The p-orbitals of the tin atoms may be occupied by these electrons results in the formation of a complex that controls the nanoparticle growth while annealing the precipitate.

Most of the researchers characterized the final product, SnO_2 NPs, rather than the intermediate-precipitated product before calcination. It appraises that the characterization of the intermediate product (colloidal hetero-crystal) may indicate the reaction mechanism involved during the formation of stannic oxide (SnO_2) at a certain temperature. Some researchers (Elango et al., 2015; Hong and Jiang, 2017; "Konstantin Stanislavsky – Bella Merlin – Google Books," n.d.) explained various bio-based precursors as reducing agents and annealed the intermediate product from 50 to 80℃; however, it is incredible to oxidize Sn(0) into SnO_2 under the stated conditions. The phenomena behind the concept can be described through Scheme 2, where biological substrates are used as complex-forming agents (or ligands) that may be decomposed easily at lower temperatures producing tin hydroxides and their oxides. Moreover, the as-prepared metal oxide NPs may be coated with a layer of organic ligand molecules at the precipitation stage. These colloidal hetero-nanocrystals are further converted to SnO_2 NPs through proper centrifugation and calcination processes.

Scheme 2 Plausible reaction mechanism of SnO_2 NPs synthesis in the presence of a reducing agent (*7-hydroxy-6-methoxy-2H-chromen-2-one)* obtained from *Catunaregam spinosa* extract

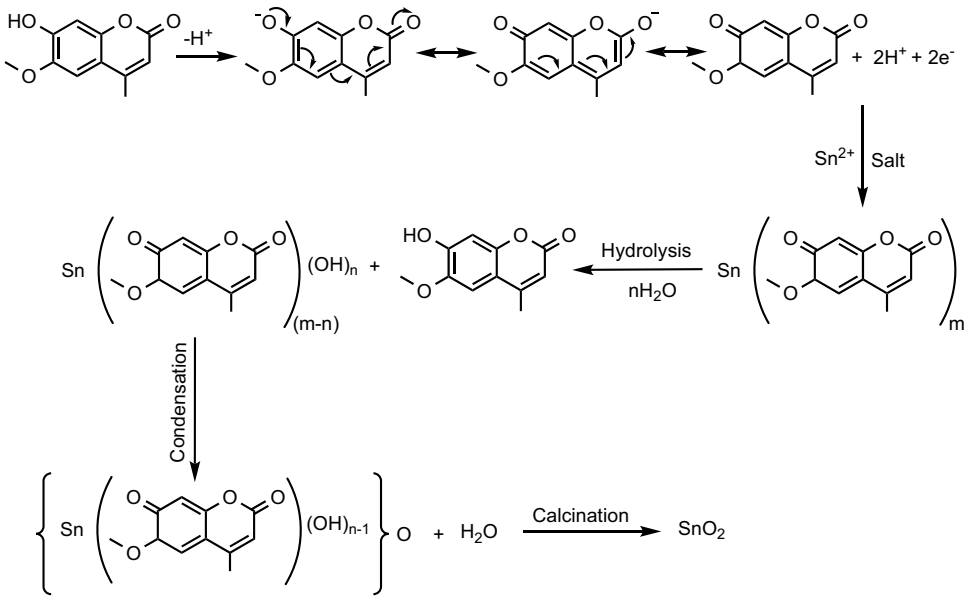

Besides, the bio-based substrates also act as capping agents to provide colloidal stability and prevent agglomeration during the nucleation process. In addition, the effect of intermolecular and intramolecular forces, nonchemical interaction, and electrostatic consequence disposes the biological substrate results in ease of nanoparticle formation and their shape (Zhang et al., 2009a, 2009b). The size and features of the nanoparticles may be affected by the nature and types of functional groups of the reducing agents. Similar phenomena were also reported elsewhere (Drzymała et al., 2017; Sk and Yue, 2014; Tammina et al., 2018; Xiong et al., 2011).

Photocatalytic application

Nanoparticles exhibit favorable photocatalytic properties due to high capacity, selectivity, and specific adsorption en route for various waste products (Coston et al., 1995). Numerous adsorbents of nanosized metallic oxides and selectively oxides of Fe, Mn, Al, Ti, Mg, Ce, Pd, Sn, etc. are typically promising materials to uptake industrial pollutants from liquid systems (Bhattacharjee and Ahmaruzzaman, 2015b; Dauthal and Mukhopadhyay, 2013; Elango et al., 2015; Haritha et al., 2016; Van Benschoten et al., 1994) due to size quantization effect and high catalytic activities (El-Sayed, 2001). The physicochemical properties of SnO_2 as photoanodes are very crucial in dye-sensitized solar cells, which are characterized by recombination resistances, charge transport, and size distributions to a greater extent (Xi and Ye, 2010). Many scientists exposed the catalytic properties of SnO_2 NPs intended for photodegradation of organic dyes in different conditions, and pharmaceuticals and agricultural degradation are discussed as follows.

Congo red degradation

Bio-green synthesis of metal oxide NPs, especially, *Catunaregam spinosa*–mediated nanosized SnO_2, was applied for photodegradation of toxic diazo congo red dye studied by Haritha et al. (2016). Heber Multilamp Photoreactor was introduced into the system to degrade the dye at 365 nm. The as-prepared SnO_2 NPs were placed in the photoreactor, followed by mixing well with congo red (1×10^{-4} M) and investigating the samples thru UV/visible spectroscopy for 5-min intervals. When SnO_2 NPs were introduced into the system, the peaks corresponding to azo dye were started to degrade and completely disappeared within 20 min. The experiment results in the rate constant of dye degradation (92%) to be $k=0.0952\times10^{-3}$ min^{-1} and kinetic data fitted with pseudo-first-order model in good agreement that relies at a time on increases C/C_0 (concentration ratio at any time to initial) decreases (Haritha et al., 2016). Hong et al. (2017) also analyzed the photocatalytic activity of SnO_2 NPs formed from the biological source of *Litsea cubeba* fruit. A glass-made batch reactor of circular shape together with a source of UV light, e.g., mercury vapor lamp, was employed for the degradation system. In general, the NPs were dispersed in congo red dye solution to ameliorate the catalytic effect in a photocatalytic process (Viju Kumar and Prem, 2018). The photodegradation of the dye typically examined by the UV/visible spectra points out that dye absorption peak is a function of annealing temperature and they are inversely proportionated. The reason behind the extensive catalytic activity of SnO_2 nanomaterial (annealed at 600℃ during synthesis) might be owing to effective surface area (26.14 m^2g^{-1}), and better interaction of the dye molecules on the catalyst surfaces reported elsewhere (Viju Kumar and Prem, 2018).

Phenol red degradation

Elango et al. (2015) showed photodegradation of organic dyes, especially phenolsulfonphthalein (commercially known as phenol red), tarnished by SnO_2 NPs prepared from the seed of *Persia americana* (Elango et al., 2015). Nearly 1×10^{-3} L of phenol red (1×10^{-4} M) in addition to 2.5×10^{-4} g SnO_2 NPs was transferred to a UV chamber to carry out the photochemical reaction at 365 nm in the visible light region. The surface plasmon resonance (SPR) of dye degradation was detected evidently at 426 nm, and the SPR band was disappeared within 2 h, proving that catalytic activity of the nanoparticles under UV light irradiation is predominant (Tammina and Mandal, 2016).

Methylene blue degradation

Photocatalytic activity of methylene blue dye was carried out thru the preparation of SnO_2 NPs from amino acid arginine reported by Bhattacharjee et al. (2015). After SnO_2 addition, the absorption band of the dye degradation decreased with the exposure time of irradiation (Bhattacharjee and Ahmaruzzaman, 2015b). The absorption band was almost disappeared at 663 nm within 4 h, and the dye solution was faded away in succession (Bhattacharjee and Ahmaruzzaman, 2015b). The rate constant of photodegradation of methylene blue was obtained, $k=1.3\times10^{-2}$ min^{-1}. The dye degradation efficiency of methylene blue was found to be 96.4% within 4 h of solar irradiation (Bhattacharjee and Ahmaruzzaman, 2015b).

Violet 4 BSN dye degradation

Tammina and Mandal (2016) exhibited remarkable photocatalytic activity of SnO_2 NPs prepared from amino acid tyrosine for Violet 4 BSN dye. The dye, commercially known as V4BSN/Acid Violet 3, was irradiated with UV

light (125 W, 254 nm). The quartz tube was operated at constant time intervals in the visible light expanse (554 nm) after being filled it with an aqueous solution of V 4 BSN dye (25 mgL^{-1}) and SnO_2 NPs (10 mg) (Drzymała et al., 2017). During photodegradation, it was witnessed to perceive complete reduction of the dye molecules through a change in color over UV exposure for 40 min. Additionally, total organic carbon (TOC) measures the rate of degradation results in 83.30% TOC that was degraded after 80 min of UV irradiation, and finally, the process reached a steady state after 2 h (Drzymała et al., 2017).

Photocatalytic activity of SnO_2 NPs for various dyes under different irradiation sources is summarized in Table 3. Particularly, violet 4 BSN dye shows 100% degradation in 40 min under 125 W UV lamp; whereas, methylene blue demonstrates excellent photodegradation for solar irradiation, and the additional results are comparable to them. In fact, photodegradation of dyes is a function of various factors, for example, source and intensity of radiation, exposure time, reaction kinetics, surface properties of the catalysts, and process temperature.

Pharmaceutical degradation

Pharmaceuticals are present in medicines, over-the-counter therapeutic, and veterinary drugs. There are available active natural or synthetic chemicals which can be absorbed into the bloodstream even at low concentrations and persist in the body for full therapeutic effects (Mezzelani et al., 2018). They are classified as (i) antibiotics, e.g., nitrofurantoin, levofloxacin, and chloramphenicol; (ii) antiviral, e.g., Tamiflu and zanamivir; (iii) antidepressant, e.g., alprazolam; (iv) antiepileptic, e.g., felbamate and carbamazepine; (v) analgesic, e.g., acetaminophen, Ibuprofen, and naproxen; and (vi) hormonal, e.g., estriol and 17-β Estradiol (Cuervo Lumbaque et al., 2019). Sources of pharmaceutical contamination to the environment include municipal wastewater, improper disposal of drugs, human excretion, intensive livestock farming, and effluents from hospitals and pharmaceutical industries (Mezzelani et al., 2018; Patel et al., 2019). These contaminants need to be removed from wastewater to protect our environment from the adverse effect of continuous exposure to pharmaceutical drugs in water (Patel et al., 2019).

Much work has been conducted to investigate pharmaceutical degradation which often involves simulation of a real wastewater treatment plant. Current process plants are equipped for the removal of simple organic substances and particulate materials at a macro/micro-scale. A large number of pharmaceutical drugs are, however, very soluble in water and mobile and are easily integrated into the general environment, even at nanoscale levels, making them hard to remove (Majumder et al., 2019).

Advanced oxidation processes (AOPs) rather than conventional methods are becoming attractive alternative techniques because of higher chances of production of harmless byproducts during pharmaceutical degradation. The fundamentals of advanced technology in water treatment for pharmaceutical compounds is the production of highly reactive species that may generate through irradiation by external energy sources like solar, ultraviolet (UV) light, visible light, microwave, or other energy sources like electricity and sound or addition of oxidizing agents. Advanced processes based on UV include photocatalysis (e.g., SnO_2/TiO_2/UV), sulphate/UV, ozonation/UV, peroxide/UV, Fenton/UV, and UV/ultrasound aimed at degrading and mineralizing organic contaminants (Serpone et al., 2017). Although the new trends of emerging these processes result in more effective degradation of organics, the new trends are rather expensive operationally. Velempini et al. (2021) studied various modified and unmodified photocatalysts in heterogeneous photocatalytic degradation of pharmaceutical drugs (Velempini et al., 2021).

Up to date, a number of reviews have surveyed the treatment of pharmaceuticals using metal oxides (Gautam et al., 2020; Gusain et al., 2019), especially SnO_2 (Diallo et al., 2016), TiO_2 (Prieto–Rodriguez et al., 2012; Sarkar

Table 3 Photocatalytic activity of SnO_2 NPs for various dyes

Sl. no	Dye	Light source	Results	Ref
1	Methylene blue	Solar irradiation	96.4% within 4 h	Bhattacharjee and Ahmaruzzaman (2015b)
2	Rhodamine B	250 W Hg lamp (≥ 365 nm)	Excellent photocatalytic activity	Wu et al. (2009)
3	Congo red	UV	Fair photocatalytic activity	Hong and Jiang (2017)
4	Rhodamine B	UV	94% degradation after 1 h	Sangami and Dharmaraj (2012)
5	Methylene blue, eosin Y, Congo red	UV	50% degradation after 20–30 min	Diallo et al. (2016)
6	Congo red	Multilamp Photoreactor (365 nm)	Pseudo 1st order; $k = 0.0952 \times 10^{-3}$ min^{-1}	Haritha et al. (2016)
7	Violet 4 BSN	125 W UV lamp (254 nm)	100% degradation of the dye in 40 min	Tammina and Mandal (2016)

et al., 2014), doped TiO_2 (Varma et al., 2020), metal–organic frameworks (MOFs), and SnO_2-based photocatalysts (Mohammad et al., 2021) for photocatalytic oxidation of organic contaminants. Recently, Velempini et al. (2021) have proposed a compound parabolic collector (CPC) that ensures high degradation efficiencies of pharmaceutical drugs through maximizing the harness of solar energy (Velempini et al., 2021). Predominantly, degradation of amoxicillin trihydrate was investigated over parabolic trough collector (PTC) which is a more advanced technological method than CPC (Dixit et al., 2016). In pilot studies, a number of common strategies to improve degradation efficiencies are adopted, i.e., combining different AOPs, dye sensitizations of metal oxides, and the addition of reagents to contaminated wastewater. Oxidative removal of diclofenac, for example, is possible when a dye is used as a photosensitizer to amplify the rate of photon absorption of SnO_2 at pilot levels with a capacity of 7.7 L for a single reactor (Diaz-Angulo et al., 2020).

Agricultural degradation

Agricultural degradation, especially soil erosion and water pollution, means a decline in soil and water conditions caused by improper use of chemicals or poor management. The utilization of various chemical fertilizers, herbicides, and insecticides in agricultural fields has led to soil pollution, and the accumulation of such toxic chemicals in water bodies is a serious threat to the aquatic ecosystem and human health (Anju and Sarita, 2010; Singh et al., 2018). Particularly, carbofuran and imidacloprid are the common insecticides utilized on a large scale in agricultural fields. They are neonicotinoid types of insecticides, being the most toxic broad-spectrum and high stability in the aquatic environment (Mishra et al., 2020; Tiˇsler et al., 2009). Prolonged exposure to these hazardous substances, including fertilizers (e.g., urea, TSP, and DAP) and herbicides (e.g., atrazine, cynazine, hexazinone, metribuzin), are detrimental to mammals, birds, fish, wildlife, as well as humans due to their anticholinesterase activity (Otieno et al., 2010; Campbell et al., 2004). They may cause serious reproductive disorders, endocrine disruption, and cytotoxic and genotoxic abnormalities in humans (Mishra et al., 2020). Therefore, the design and development of effective state-of-the-art technologies to eradicate such xenobiotics from soil and water is of utmost significance to the aquatic ecosystem and public health (Bolong et al., 2009).

The addition of nanomaterials in agriculture is to reduce the extent of chemicals, minimize nutrient losses in fertilization, and increase yield through pest and nutrient management. Mahanta and Ahmaruzzaman (2021) demonstrated a cost-effective hydrothermal technique designed for the fabrication of SnO_2-based novel nanohybrids, e.g., Fe_3O_4-SnO_2-gC_3N_4 and Au-SnO_2-CdS, with a view to the photodegradation of the toxic chemicals (Mohanta and Ahmaruzzaman, 2021a, 2021b). The heterojunctions showed sound photocatalytic degradation against emerging pollutants like carbofuran and imidacloprid under LED irradiation with a degradation efficiency up to ~ 95%. In fact, superoxide anion radical has been reported to be the major reactive oxygen species. The visible light absorption ability of Fe_3O_4, Au, CdS, etc., followed by the heterojunction structures of energy levels to hinder charge recombination, facilitates enhanced LED light-induced photocatalytic degradation of the organic pollutants. Prasad et al. (2017) reviewed nanotechnology in sustainable agriculture that includes specific applications like nanofertilizers and nanopesticides to trail levels of products and nutrients to increase the productivity without decontamination of soil, water, and protection against some insect pest and microbial diseases (Prasad et al., 2017).

Mechanism of dye degradation

Organic dye degradation by means of SnO_2 NPs is the most common application, and corresponding photodegradation perception is available in the literature. Nonetheless, the mechanism of photocatalytic activity, still an open question, mostly depends upon the free radical generation simultaneously either from the excited dye molecules or/and nanoparticles exposed to UV/visible irradiation.

Firstly, the electrons produced from the free radicals of dye molecules are got excited into singlet and triplet states. The electrons were injected into the conduction band (e_{CB}^-) of the photocatalyst prior to the formation of cationic dye radicals (dye^+) (Nilavazhagan et al., 2014). SnO_2 NPs as dye-sensitized photocatalysts react with atmospheric oxygen to form oxidizing species ($O_2{}^{*-}$, HOO*, and *OH radicals) which are effective towards oxidization of the dye effluents. The probable reaction scheme for the degradation of organic dyes by means of SnO_2 NPs was discussed by Bhattacharjee et al. (2016) as follows, and the mechanism is shown in Fig. 6 (Nilavazhagan et al., 2014):

$$Dye + h\nu \rightarrow Dye^*$$
$$Dye^* + SnO_2 \rightarrow Dye^{*+} + SnO_2(e_{CB}^-)$$
$$SnO_2(e_{CB}^-) + O_2 \rightarrow O_2^{*-} + SnO_2$$
$$O_2^{*-} + H^+ \rightarrow OOH^+$$
$$OOH^+ + O_2^{*-} + H^+ \rightarrow O_2 + H_2O_2$$
$$H_2O_2 + O_2^{*-} \rightarrow OH^* + OH^- + O_2$$
$$Dye^{*+} + OH^* \rightarrow Degradation\_products$$
$$Dye^{*+} + O_2^{*-} \rightarrow Degradation\_products$$
$$Dye^{*+} + O_2 \rightarrow Degradation\_products$$

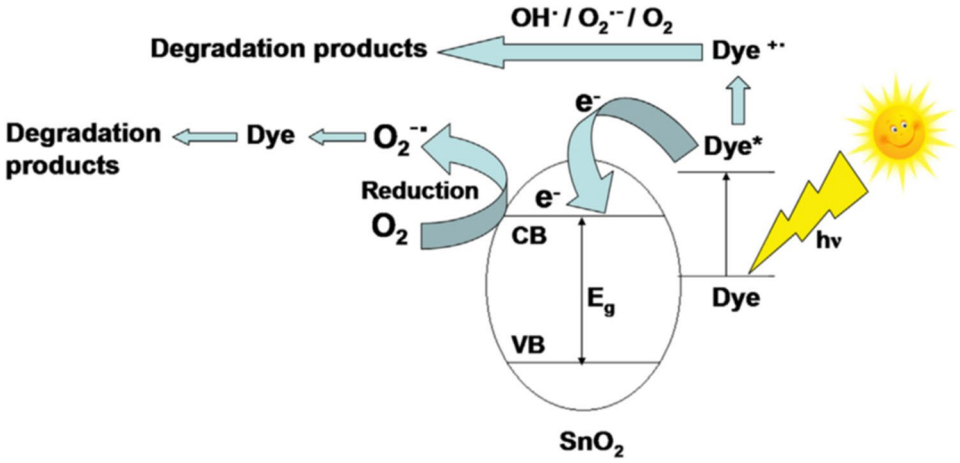

Fig. 6 Probable mechanism of dye degradation using dye-sensitized SnO_2 photocatalyst under direct sunlight (dye molecules excited first) (Nilavazhagan et al., 2014)

Secondly, SnO_2 NPs are exposed to irradiation; electrons get excited and generate holes (h^+) spontaneously in the valence band (VB) located below the Fermi energy level (FEL). Electron acceptors, e.g., surface oxygen species (O_2), readily capture the as-generated photoelectrons (e^-) results in the production of superoxide free radicals (O_2^{*-}). It is noted that during dye degradation, the number of photoelectrons (e^-) is proportional to that of the free radicals (O_2^{*-}). Consequently, the holes are trapped by electron donors, for instance, surface water or organic effluents, and ultimately reduced. Holes are a strong oxidizing agent that generally influences the oxidizing power of photogenerated holes. As a result, photogenerated electrons (e^-) and holes (h^+) competitively separate and recombine during the photochemical reaction, finding out the fact that these electrons constrain the recombination of e^- and h^+ on the surface of the photocatalyst in line for oxygen vacancies or existence of surface defects (Liqiang et al., 2006). An alternative hypothetical mechanism of the photocatalysis system has been illustrated in Fig. 7.

Photocatalytic activity of SnO_2 NPs towards photodegradation of hazardous dyes under UV/visible irradiation exclusively depends upon a number of factors, e.g., particle size, bandgap, defects, and dosage of the catalysts. Bandgap plays a vital role in dye degradation. Semiconductor NPs, in general, influence quantum confinement features, i.e., bandgap energy is inversely related to particle size focusing on nanoparticles with lower crystallite size that shows a higher rate of dye degradation or requires time shorter enough (Bhattacharjee and Ahmaruzzaman, 2015b). Besides, particle size is a function of temperature as well as bandgap (Babar et al., 2010; Celina Selvakumari et al., 2018; Tammina et al., 2018). Tammina et al. (2018) investigated the effect of temperature on crystallite size of the SnO_2 NPs and calculated corresponding bandgaps from *Tauc* plots (Fig. 8) (Tammina et al., 2018). The bandgap values obtained to be

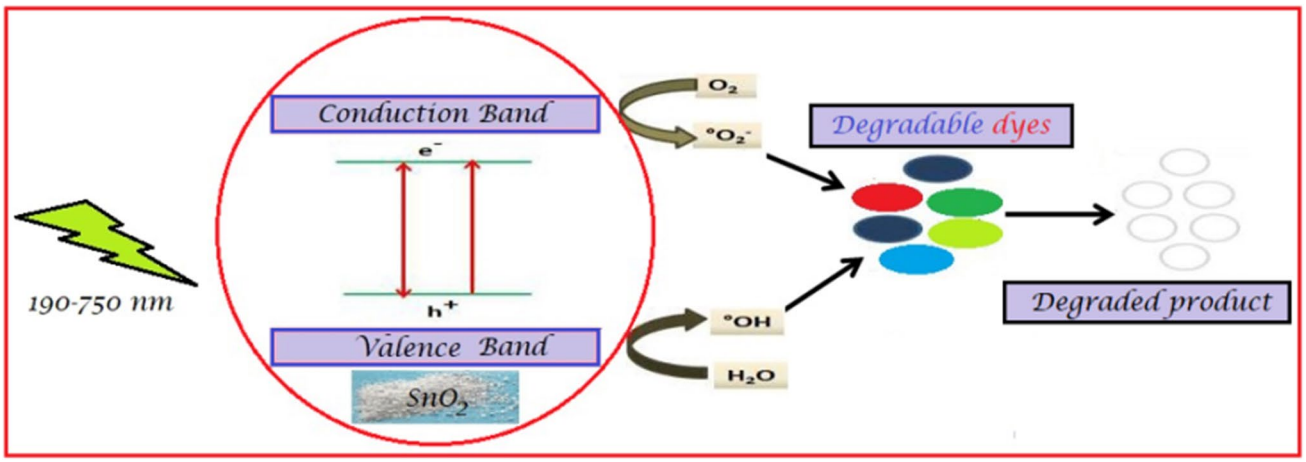

Fig. 7 Hypothetical mechanism of dye degradation using dye-sensitized SnO_2 photocatalyst under direct sunlight (SnO_2 NPs excited first)

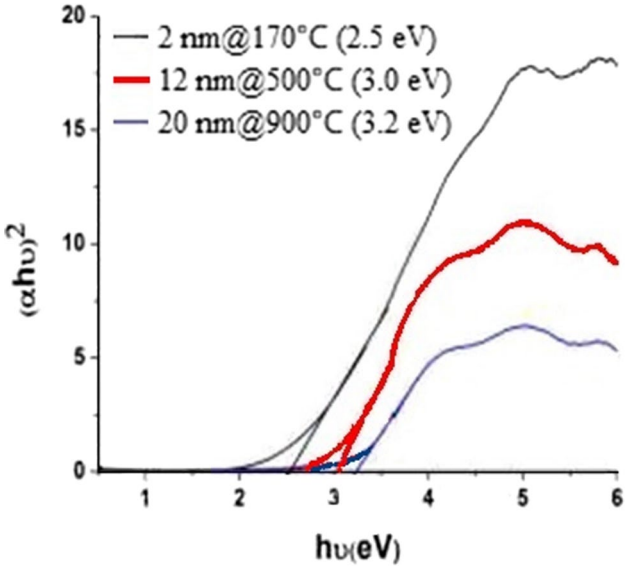

Fig. 8 *Tauc* plots of SnO_2 NPs of crystallite size 2 nm calcined at 170℃ (bandgap 2.5 eV), 12 nm at 500℃ (bandgap 3.0 eV), and 20 nm at 900℃ (bandgap 3.2 eV) (Tammina et al., 2018)

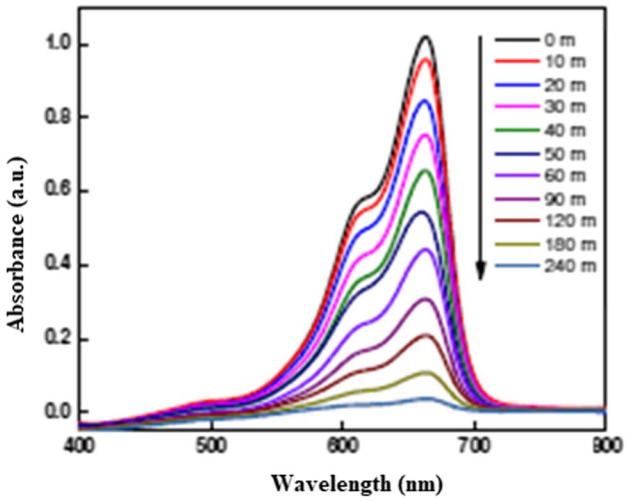

Fig. 9 Photodegradation of methylene blue dye by solar radiation using SnO_2 NPs (Bhattacharjee and Ahmaruzzaman, 2015b)

2.5 eV, 3.0 eV, and 3.2 eV of the as-prepared samples were calcined to produce crystallite size ~ 2 nm at 170℃, ~ 12 nm at 500℃, and ~ 20 nm at 900℃, respectively. The decrease in bandgap from the standard value of 3.6 eV is attributed to the crystal defects, leading to come-off electronic transitions from VB to FEL (Diallo et al., 2016). These defects create oxygen vacancies as well as generate charge carriers that contribute to reduce the rate of electron–hole recombination on the catalyst surface (Esmaielzadeh Kandjani et al., 2010). In parallel, free radicals may be generated by the charge carriers through the reaction between absorbed O_2 and H_2O on the surface; the additional reaction may achieve with these free radicals and dye molecules to form azo bonds in the direction of degradation or mineralization of dyes discussed earlier.

Furthermore, SnO_2 NPs alter the absorption band of the dye molecules, and this band decreases with the exposure time of irradiation over catalyst addition. It has been reported that particle size is an important factor that strongly influences the adsorption of dyes and smaller size NPs enhance interaction between the macro-molecules and free radicals created on the surface (Bhattacharjee and Ahmaruzzaman, 2015b; Jiang et al., 2008; Suttiponparnit et al., 2010). Bhattacharjee et al. (2015) reported that the absorption band of methylene blue almost disappeared within 4 h after the addition of SnO_2 NPs at 663 nm of irradiation (Fig. 9) (Bhattacharjee and Ahmaruzzaman, 2015b) results in the reduction of the complex dye structure of chromophore. Haritha et al. (2016) inferred almost similar findings point out that congo red dye showed strong degradation (92%) of a high-intensity peak at 502 nm for 20 min by using the nanoparticles (Haritha et al., 2016). In fact, dye degradation with various nanoparticles is a subject of different conditions, e.g., catalyst/dye ratio, radiation source, synthetic methods, and irradiation time, presented in Table 4.

This assessment revealed that SnO_2 NPs prepared basically from ascorbic acid exhibited strong photocatalytic activities (Tammina et al., 2018). Besides, various creative findings have been reported in the literature on nanocomposites of SnO_2 that enhance remarkable visible-light-induced photodegradation of organic contaminants from wastewater (Mohanta et al., 2018; Mohanta and Ahmaruzzaman, 2021c, 2021b, 2021a). Likewise, heterojunction nanocomposites (Cu/ZnO, Pd/ZnO, etc.) demonstrated better results (~100% dye degraded) (Momeni et al., 2016a, 2016b) than the rest reported in Table 4. The reason behind the higher degradation rate of dye molecules with reduced size of SnO_2 NPs has been reported that molecules with higher molar absorptivity are more stable and establish surface plasmon resonance (Heger et al., 2005).

Technological challenges

Integration of nanotechnology with bio-resources towards practical application is of current challenges in the field of nanoparticle synthesis and utilization (Chen et al., 2014). The focal point of the biosynthesis of SnO_2 NPs is to develop traditional methods as well as create biodegradable materials from available green resources which are nontoxic, cost-effective, and environmentally benign in nature.

To produce SnO_2 NPs through the bio-reduction procedure at moderate temperature and pH yields controlled

Table 4 Comparison of azo dye degradation by various NPs in different conditions

Material	Dye	Catalyst/dye ratio	Radiation source/method	Irradiation time (min)	Degradation (%)	Reference
SnO_2	Methylene blue	22.20	UV lamp	180	79	Kim et al. (2016)
SnO_2/SnO	Methylene blue	50.00	UV lamp	180	90.28	Song and Kang (2000)
SnO_2	Methylene blue	26.67	UV lamp	120	90	Vatanparast and Taghizadeh (2016)
SnO_2	Methylene blue	28.57	UV lamp	30	90	Tammina et al. (2018)
TiO_2	Congo red	–	Solar radiation	–	69	Ljubas et al. (2015)
CeO_2/Nylon	Congo red	–	Solution casting	–	96	Latha et al. (2016)
Au	Congo red	–	Self-reduction	–	95	Subair et al. (2016)
Cu/ZnO	Congo red	–	Green synthesis	–	100 at 5th cycle	Kim et al. (2016)
Co–Ni	Congo red	–	Microwave	–	90–96.8 at various pH	Liu et al. (2016)
Cu	Congo red, methylene orange	–	In situ preparation	–	75	Kamal et al. (2016)
WO_3	Congo red	–	Surfactants as capping agents	–	95	Shukla et al. (2016)
ZnO	Congo red	–	Microwave hydrothermal	–	43	Vatanparast and Taghizadeh (2016)
Pd/ZnO	Congo red	–	Microwave hydrothermal	–	98	Vatanparast and Taghizadeh (2016)
SnO_2	Congo red	–	UV multilamp	20	92	Haritha et al. (2016)

particle size, there should be an improvement in the surface morphology and crystallographic properties. In order to enhance the feasibility of chemical precipitation methods in the future, extensive efforts are needed to overcome some technological challenges.

Firstly, chemical precipitation methods involve the complexity of the process and frequently required high temperature which results in large-grain sizes. At times, this method includes some toxic chemicals a threat to the environment (Chen et al., 2014).

Secondly, an inevitable introduction of byproducts shows the supplementary problem with the methods which require subsequent purification steps. As a result, such processes are time-consuming and entail extra costs (Seabra and Durán, 2015).

Thirdly, in the literature, there are plenty of studies on the removal of organic pollutants; most of them have used dyes as model contaminants for the treatment process. These dyes can simply be removed in comparison to some other organic products, such as pesticides and endocrine-disrupting compounds. However, a deeper understanding is required for a state-of-the-art mechanism of dye degradation and plausible interaction with organic pollutants containing complex molecular structures.

Fourthly, most of the researchers used tin chlorides ($SnCl_2$ or $SnCl_4$) to synthesize SnO_2 NPs owing to cost-effective, available, and easy handling properties. Nevertheless, the fact behind the studies is the difficulty to remove chloride ions from the system, and it badly affects the superficial and electrical features of the material (Thamarai Selvi and Meenakshi Sundar, 2018). The chloride tricky can be removed through the usage of organic tin compounds, such as alkoxides, but these reagents are quite expensive which makes their industrial implementation hardly possible.

Fifthly, further improvement is still a current demand in the preparation of nanomaterials. There are three key factors, e.g., reaction medium, capping, and reducing agents, which must be sincerely designed from the green chemistry and economic viewpoints for the synthesis and stabilization of nanoparticles. Additional needs to be investigated the quality and performance of SnO_2 NPs based on biological substrates, as the chemicals used are quite costly when chemical precipitation methods are chosen.

Finally, even if the application of metal oxide NPs is increasingly tremendous in various fields, including water treatment, food technology, medicine, and agriculture, but still there are some adverse effects of the NPs on the health of living organisms (Chen et al., 2014; Galdiero et al., 2011). There are various studies on the toxicity of metal oxide NPs, and there is also a rising trend in the cytotoxic potential of these nanoparticles (Carmona–Quiroga et al., 2021; Seabra and Durán, 2015). Recently, Lang et al. (2021) reviewed sustainable smart technology of biosynthesis of nanomaterials to utilize their beneficial effects devoid of posing a threat to living entities. It is a global challenge of preparing ecologically benign SnO_2 NPs with better efficiency and minimum toxic effect on humans and to the environment towards sustainability. Therefore, future research must be conducted,

suggesting that a series of standard safety evaluations and toxicological risk assessment associated with metal oxide NPs synthesis, characterization, distribution, and environmental emission towards practical application.

Conclusion

There is a current lacking in a review article on the biosynthesis of SnO_2 NPs through the chemical precipitation method; nevertheless, huge studies report the possibility of obtaining SnO_2 NPs from bio-resources accompanied by photocatalytic application of the NPs. The method is interesting, thanks to nontoxic, cost-effective, and eco-friendly approaches, but it still remains a challenge due to a number of factors that possess a barrier to the elucidation of the reactions and mechanism of formation. Hence, the review includes a summary of various capping or reducing agents extracted from biological substrates and methodologies applied to the synthesis. The substrate found in abundance from the extract of root bark of *Catunaregam spinosa* is chromenone compound ($C_{10}H_8O_3$) that has been recommended as a model complex-forming agent (or ligand) for the transformation of metal salts into SnO_2 NPs, and a promising reaction mechanism has been discussed. Besides, photodegradation of dyes, pharmaceuticals, and agricultural contaminants over SnO_2 NPs has been discoursed, and according to the literature review, it has been reported that the photocatalytic activity mainly depends upon the mechanism of free radical generation during UV/visible irradiation. In fact, the bio-reduction mechanism of the nanoparticle formation and photocatalytic degradation features of the metal oxide has still to be defined and understood due to the high complexity of the biological extracts and thermodynamically stable structures of dyes, respectively. With the considerable progress over the last few years and clear goals that emerged from the study, a sensible increase in research on the subject matter and related fields is expected in the near future.

Author contribution Sumaya Tarannum Nipa and Rumana Akter are responsible for literature review and writing the synthetic part of the article; Md. Al Raihan and Sk. Shahriar bin Rasul have discussed the bio-reduction mechanism of nanoparticle formation and photocatalytic dye degradation features; Uday Som, Shafi Ahmed, and Md. Jahangir Alam collected data and structure of the article; Md. Maksudur Rahman Khan and Stefano Enzo are responsible for the revision, review, and structure of the article; Md. Wasikur Rahman planned and directed for writing the article, the research of the structure, the collection of data, and overall reviewing.

Funding This research did not receive any specific grant from funding agencies in the public, commercial, or not-for-profit sectors.

Availability of data and materials Not applicable.

Declarations

Ethics approval No ethical issues.

Consent to participate Consent.

Consent for publication Consent.

Competing interests The authors declare no competing interests.

References

Agrahari V, Mathpal MC, Kumar M, Agarwal A (2015) Investigations of optoelectronic properties in DMS SnO_2 nanoparticles. J Alloy Compd 622:48–53. https://doi.org/10.1016/j.jallcom.2014.10.009

Ahmad S, Wijaya K, Trisunayati W S (2016) Journal of. Asian Journal of Chemistry 28, 347–350. https://doi.org/10.1093/jae/ejm029

Ajoudanian N, Nezamzadeh-Ejhieh A (2015) Enhanced photocatalytic activity of nickel oxide supported on clinoptilolite nanoparticles for the photodegradation of aqueous cephalexin. Mater Sci Semicond Process 36:162–169. https://doi.org/10.1016/j.mssp.2015.03.042

Anju TJ, Sarita S (2010) Suitability of Foxtail Millet (Setaria italica) and Barnyard Millet (Echinochloa frumentacea) for development of low glycemic index biscuits. Malays J Nutr 16:361–368

Arularasu MV, Anbarasu M, Poovaragan S, Sundaram R, Kanimozhi K, Magdalane CM, Kaviyarasu K, Thema FT, Letsholathebe D, Mola GT, Maaza M (2017) Structural, optical, morphological and microbial studies on SnO_2 nanoparticles prepared by co-precipitation method. J Nanosci Nanotechnol 18:3511–3517. https://doi.org/10.1166/jnn.2018.14658

Ashour NI (2018) Fabrication of SnO_2 Q-dot thin films using ultrasonic spray techniques for optoelectronics applications. Int J Appl Eng Res 13:1071–1074. http://www.ripublication.com

Babar AR, Shinde SS, Moholkar AV, Rajpure KY (2010) Electrical and dielectric properties of co-precipitated nanocrystalline tin oxide. J Alloy Compd 505:743–749. https://doi.org/10.1016/j.jallcom.2010.06.131

Bakrania SD, Wooldridge MS (2009) The effects of two thick film deposition methods on tin dioxide gas sensor performance. Sensors 9:6853–6868. https://doi.org/10.3390/s90906853

Balzani V (2005) Nanoscience and nanotechnology: a personal view of a chemist. Small 1:278–283. https://doi.org/10.1002/smll.200400010

Batzill M, Katsiev K, Diebold U (2003) Surface morphologies of SnO_2(110). Surf Sci 529:295–311. https://doi.org/10.1016/S0039-6028(03)00357-1

Batzill M, Kim J, Beck DE, Koel BE (2004) Epitaxial growth of tin oxide on Pt(111): structure and properties of wetting layers and crystallites. Phys Rev B 69

Begum S, Ahmaruzzaman M (2018) CTAB and SDS assisted facile fabrication of SnO_2 nanoparticles for effective degradation of carbamazepine from aqueous phase: a systematic and comparative study of their degradation performance. Water Res 129:470–485. https://doi.org/10.1016/j.watres.2017.11.031

Begum S, Devi TB, Ahmaruzzaman M (2016) L-lysine monohydrate mediated facile and environment friendly synthesis of SnO_2 nanoparticles and their prospective applications as a catalyst for the reduction and photodegradation of aromatic

compounds. J Environ Chem Eng 4:2976–2989. https://doi.org/10.1016/j.jece.2016.05.024
Beydoun D, Amal R, Low G, McEvoy S (1999) Role of nanoparticles in photocatalysis. J Nanopart Res 1:439–458. https://doi.org/10.1023/A:1010044830871
Bhattacharjee A, Ahmaruzzaman M (2015a) Facile synthesis of SnO_2 quantum dots and its photocatalytic activity in the degradation of eosin Y dye: a green approach. Mater Lett 139:418–421. https://doi.org/10.1016/j.matlet.2014.10.121
Bhattacharjee A, Ahmaruzzaman M (2015b) A green and novel approach for the synthesis of SnO_2 nanoparticles and its exploitation as a catalyst in the degradation of methylene blue under solar radiation. Mater Lett 145:74–78. https://doi.org/10.1016/j.matlet.2015.01.029
Bhattacharjee A, Ahmaruzzaman M (2015d) Photocatalytic–degradation and reduction of organic compounds using SnO_2 quantum dots (via a green route) under direct sunlight. RSC Adv 5:66122–66133. https://doi.org/10.1039/c5ra07578e
Bhattacharjee A, Ahmaruzzaman M, Sinha T (2014) Surfactant effects on the synthesis of durable tin-oxide nanoparticles and its exploitation as a recyclable catalyst for the elimination of toxic dye: a green and efficient approach for wastewater treatment. RSC Adv 4:51418–51429. https://doi.org/10.1039/C4RA08461F
Bhattacharjee A, Ahmaruzzaman M, Sinha T (2015) A novel approach for the synthesis of SnO_2 nanoparticles and its application as a catalyst in the reduction and photodegradation of organic compounds. Spectrochim Acta Part A Mol Biomol Spectrosc 136:751–760. https://doi.org/10.1016/j.saa.2014.09.092
Bhattacharjee A, Ahmaruzzaman M, Devi TB, Nath J (2016) Photodegradation of methyl violet 6B and methylene blue using tin-oxide nanoparticles (synthesized via a green route). J Photochem Photobiol, A 325:116–124. https://doi.org/10.1016/j.jphotochem.2016.03.032
Bolong N, Ismail AF, Salim MR, Matsuura T (2009) A review of the effects of emerging contaminants in wastewater and options for their removal. Desalination 239:229–246. https://doi.org/10.1016/j.desal.2008.03.020
Campbell S, David MD, Woodward LA, Li QX (2004) Persistence of carbofuran in marine sand and water. Chemosphere 54:1155–1161. https://doi.org/10.1016/J.CHEMOSPHERE.2003.09.018
Cao H, Qiu X, Liang Y, Zhang L, Zhao M, Zhu Q (2006) Sol-gel template synthesis and photoluminescence of n- and p-type semiconductor oxide nanowires. Chem Phys Chem 7:497–501. https://doi.org/10.1002/cphc.200500452
Carmona-Quiroga PM, Montes M, Pato E, Fernández-Jiménez A, Blanco-Varela MT (2021) Study on the activation of ternesite in $CaO{\cdot}Al_2O_3$ and $12CaO{\cdot}7Al_2O_3$ blends with gypsum for the development of low-CO_2 binders. J Clean Prod 291:125726. https://doi.org/10.1016/j.jclepro.2020.125726
Celina Selvakumari J, Nishanthi ST, Dhanalakshmi J, Ahila M, Pathinettam Padiyan D (2018) Bio-active synthesis of tin oxide nanoparticles using eggshell membrane for energy storage application. Appl Surf Sci 441:530–537. https://doi.org/10.1016/j.apsusc.2018.02.043
Chandra Bose A, Kalpana D, Thangadurai P, Ramasamy S (2002) Synthesis and characterization of nanocrystalline SnO_2 and fabrication of lithium cell using nano-SnO_2. J Power Sources 107:138–141. https://doi.org/10.1016/S0378-7753(01)00995-8
Chang JS, Strunk J, Chong MN, Poh PE, Ocon JD (2020) Multidimensional zinc oxide (ZnO) nanoarchitectures as efficient photocatalysts: what is the fundamental factor that determines photoactivity in ZnO? J Hazard Mater 381:120958. https://doi.org/10.1016/j.jhazmat.2019.120958
Chappel S, Zaban A (2002) Nanoporous SnO_2 electrodes for dye-sensitized solar cells: improved cell performance by the synthesis of 18nm SnO_2 colloids. Sol Energy Mater Sol Cells 71:141–152. https://doi.org/10.1016/S0927-0248(01)00050-2
Chen W, Zhou Q, Wan F, Gao T (2012) Gas sensing properties and mechanism of nano-SnO_2-based sensor for hydrogen and carbon monoxide. J Nanomater 2012:612420. https://doi.org/10.1155/2012/612420
Chen H, Zhang D, Zhou X, Zhu J, Chen X, Zeng X (2014) Controllable construction of ordered porous SnO_2 nanostructures and their application in photocatalysis. Mater Lett 116:127–130. https://doi.org/10.1016/j.matlet.2013.10.111
Cheng B, Russell JM, Shi Zhang L, Samulski ET (2004) Large-scale, solution-phase growth of single-crystalline SnO_2 nanorods. Journal of the American Chemical Society 126:5972–5973. https://doi.org/10.1021/ja0493244
Cho S, Yu J, Kang SK, Shih D-Y (2005) Oxidation study of pure tin and its alloys via electrochemical reduction analysis. Journal of Electronic Materials 34:635–642. https://doi.org/10.1007/s11664-005-0077-6
Chu G, Zeng Q, Shen Z, Zou H, Chen J (2014) Preparation of SnO_2 nanoparticles using a helical tube reactor via continuous hydrothermal route. Chem Eng J 253:78–83. https://doi.org/10.1016/j.cej.2014.05.016
Cocco G, Enzo S, Carturan G, Orsini PG, Scardi P (1987) Synthesis and thermal behavior of gel-derived SnO_2-Sb_2O_5 semiconducting glaze. Mater Chem Phys 17:541–551. https://doi.org/10.1016/0254-0584(87)90013-7
Coston JA, Fuller CC, Davis JA (1995) Pb2+ and Zn2+ adsorption by a natural aluminum- and iron-bearing surface coating on an aquifer sand. Geochim Cosmochim Acta 59:3535–3547. https://doi.org/10.1016/0016-7037(95)00231-N
Cuervo Lumbaque E, Lopes Tiburtius ER, Barreto-Rodrigues M, Sirtori C (2019) Current trends in the use of zero-valent iron (Fe0) for degradation of pharmaceuticals present in different water matrices. Trends in Environmental Analytical Chemistry 24:e00069. https://doi.org/10.1016/j.teac.2019.e00069
Cusack, P.A., 1998. Book Review: Chemistry of Tin, 2nd edition, P.J. Smith (ed). Blackie Academic & Professional, London, 1997. 578 pages. ISBN 0–7514–0385–7. Applied Organometallic Chemistry 12, 520. https://doi.org/10.1002/(SICI)1099-0739(199807)12:7<520::AID-AOC747>3.0.CO;2-T
Dai ZR, Pan ZW, Wang ZL (2001) Ultra-long single crystalline nanoribbons of tin oxide. Solid State Commun 118:351–354. https://doi.org/10.1016/S0038-1098(01)00122-3
Dai ZR, Gole JL, Stout JD, Wang ZL (2002) Tin oxide nanowires, nanoribbons, and nanotubes. J Phys Chem B 106:1274–1279. https://doi.org/10.1021/jp013214r
Das RN (2001) Chemical processing of nanostructured materials. MRS Proc 676(Y3):10. https://doi.org/10.1557/PROC-676-Y3.10
Dauthal P, Mukhopadhyay M (2013) Biosynthesis of palladium nanoparticles using Delonix regia leaf extract and its catalytic activity for nitro-aromatics hydrogenation. Ind Eng Chem Res 52:18131–18139. https://doi.org/10.1021/ie403410z
Deosarkar MP, Pawar SM, Sonawane SH, Bhanvase BA (2013) Process intensification of uniform loading of SnO_2 nanoparticles on graphene oxide nanosheets using a novel ultrasound assisted in situ chemical precipitation method. Chem Eng Process 70:48–54. https://doi.org/10.1016/j.cep.2013.05.008
Derikvandi H, Nezamzadeh-Ejhieh A (2017) Increased photocatalytic activity of NiO and ZnO in photodegradation of a model drug aqueous solution: effect of coupling, supporting, particles size and calcination temperature. J Hazard Mater 321:629–638. https://doi.org/10.1016/j.jhazmat.2016.09.056
Devi P, Banerjee S, Chowdhury S, Suresh Kumar G (2012) Eggshell membrane: a natural biotemplate to synthesize fluorescent gold nanoparticles. RSC Adv 2:11578–11585. https://doi.org/10.1039/C2RA21053C

Diallo A, Manikandan E, Rajendran V, Maaza M (2016) Physical & enhanced photocatalytic properties of green synthesized SnO_2 nanoparticles via Aspalathus linearis. J Alloy Compd 681:561–570. https://doi.org/10.1016/j.jallcom.2016.04.200

Diaz-Angulo J, Lara-Ramos J, Mueses M, Hernández-Ramírez A, Li Puma G, Machuca–Martínez, F., (2020) Enhancement of the oxidative removal of diclofenac and of the TiO_2 rate of photon absorption in dye-sensitized solar pilot scale CPC photocatalytic reactors. Chem Eng J 381:122520. https://doi.org/10.1016/j.cej.2019.122520

Dixit D, Verma A, Gupta S, Bansal P (2016) Assessment of solar photocatalytic degradation and mineralization of amoxicillin trihydrate (AMT) using slurry and fixed-bed batch reactor: efficacy of parabolic trough collector. RSC Adv 6:36109–36117. https://doi.org/10.1039/C6RA03414D

Drzymała E, Gruzeł G, Depciuch J, Budziak A, Kowal A, Parlinska-Wojtan M (2017) Structural, chemical and optical properties of SnO_2 NPs obtained by three different synthesis routes. J Phys Chem Solids 107:100–107. https://doi.org/10.1016/j.jpcs.2017.03.026

Elango G, Kumaran SM, Kumar SS, Muthuraja S, Roopan SM (2015) Green synthesis of SnO_2 nanoparticles and its photocatalytic activity of phenolsulfonphthalein dye. Spectrochim Acta Part A Mol Biomol Spectrosc 145:176–180. https://doi.org/10.1016/j.saa.2015.03.033

El-Sayed MA (2001) Some interesting properties of metals confined in time and nanometer space of different shapes. Acc Chem Res 34:257–264. https://doi.org/10.1021/ar960016n

Esmaielzadeh Kandjani A, Farzalipour Tabriz M, Arefian NA, Vaezi MR, Halek F, Sadrnezhaad SK (2010) Photocatalytic decoloration of Acid Red 27 in presence of SnO_2 nanoparticles. Water Sci Technol 62:1256–1264. https://doi.org/10.2166/wst.2010.156

Fatima R, Afridi MN, Kumar V, Lee J, Ali I, Kim K-H, Kim J–O (2019) Photocatalytic degradation performance of various types of modified TiO_2 against nitrophenols in aqueous systems. Journal of Cleaner Production 231:899–912. https://doi.org/10.1016/j.jclepro.2019.05.292

Finn RD, Coggill P, Eberhardt RY, Eddy SR, Mistry J, Mitchell AL, Potter SC, Punta M, Qureshi M, Sangrador-Vegas A, Salazar GA, Tate J, Bateman A (2015) The Pfam protein families database: towards a more sustainable future. Nucleic Acids Res 44:D279–D285. https://doi.org/10.1093/nar/gkv1344

Fu Z, Yang HK, Moon BK, Choi BC, Jeong JH (2011) Hydrothermal synthesis and optical properties of Eu 3+-doped $CaSnO_3$ nanocrystals. J Nanosci Nanotechnol 11:1629–1631. https://doi.org/10.1166/jnn.2011.3384

Gaber A, Abdel-Latief AY, Abdel-Rahim MA, Abdel-Salam MN (2013) Thermally induced structural changes and optical properties of tin dioxide nanoparticles synthesized by a conventional precipitation method. Mater Sci Semicond Process 16:1784–1790. https://doi.org/10.1016/j.mssp.2013.06.026

Galdiero S, Falanga A, Vitiello M, Cantisani M, Marra V, Galdiero M (2011) Silver nanoparticles as potential antiviral agents. Molecules 16:8894–8918. https://doi.org/10.3390/molecules16108894

Gautam S, Agrawal H, Thakur M, Akbari A, Sharda H, Kaur R, Amini M (2020) Metal oxides and metal organic frameworks for the photocatalytic degradation: a review. J Environ Chem Eng 8:103726. https://doi.org/10.1016/j.jece.2020.103726

Giefers H, Porsch F, Wortmann G (2005) Kinetics of the disproportionation of SnO. Solid State Ionics 176:199–207. https://doi.org/10.1016/j.ssi.2004.06.006

Greenwood, N.N., Earnshaw, A., n.d. Chemistry of the Elements, 2nd Edition

Guo D-J (2011) Electrooxidation of ethanol on novel multi-walled carbon nanotube supported platinum-antimony tin oxide nanoparticle catalysts. J Power Sources 196:679–682. https://doi.org/10.1016/j.jpowsour.2010.07.075

Guo H, Wang Y, Li G, Liu J, Li Y (2016) The persistent energy transfer of Eu2+ and Dy3+ and luminescence properties of a new cyan afterglow phosphor α–Ca3(PO4)2:Eu2+, Dy3+. RSC Adv 6:101731–101736. https://doi.org/10.1039/C6RA19386B

Gusain R, Gupta K, Joshi P, Khatri OP (2019) Adsorptive removal and photocatalytic degradation of organic pollutants using metal oxides and their composites: a comprehensive review. Adv Coll Interface Sci 272:102009. https://doi.org/10.1016/j.cis.2019.102009

Haritha E, Roopan SM, Madhavi G, Elango G, Al-Dhabi NA, Arasu MV (2016) Green chemical approach towards the synthesis of SnO_2 NPs in argument with photocatalytic degradation of diazo dye and its kinetic studies. Journal of Photochemistry and Photobiology B: Biology 162:441–447. https://doi.org/10.1016/j.jphotobiol.2016.07.010

Heger D, Jirkovsk J, Kln P (2005) Aggregation of methylene blue in frozen aqueous solutions studied by absorption spectroscopy. J Phys Chem A 109:6702–6709. https://doi.org/10.1021/jp050439j

Hoffmann MR, Martin ST, Choi W, Bahnemann DW (1995) Environmental applications of semiconductor photocatalysis. Chem Rev 95:69–96. https://doi.org/10.1021/cr00033a004

Hong G-B, Jiang C-J (2017) Synthesis of SnO_2 nanoparticles using extracts from Litsea cubeba fruits. Materials Letters 194:164–167. https://doi.org/10.1016/j.matlet.2017.02.058

Houari M, Hamdi B, Bouras O, Bollinger J-C, Baudu M (2014) Static sorption of phenol and 4-nitrophenol onto composite geomaterials based on montmorillonite, activated carbon and cement. Chem Eng J 255:506–512. https://doi.org/10.1016/j.cej.2014.06.065

Hu JQ, Ma XL, Shang NG, Xie ZY, Wong NB, Lee CS, Lee ST (2002) Large-scale rapid oxidation synthesis of SnO_2 nanoribbons. J Phys Chem B 106:3823–3826. https://doi.org/10.1021/jp0125552

Ibarguen CA, Mosquera A, Parra R, Castro MS, Rodríguez-Páez JE (2007) Synthesis of SnO_2 nanoparticles through the controlled precipitation route. Mater Chem Phys 101:433–440. https://doi.org/10.1016/j.matchemphys.2006.08.003

Jeong K-E, Kim H-D, Kim T-W, Kim J-W, Chae H-J, Jeong S-Y, Kim C-U (2014) Hydrogen production by aqueous phase reforming of polyols over nano- and micro-sized mesoporous carbon supported platinum catalysts. Catalysis Today 232:151–157. https://doi.org/10.1016/j.cattod.2014.02.005

Jia X, Liu Y, Wu X, Zhang Z (2014) A low temperature situ precipitation route to designing Zn-doped SnO_2 photocatalyst with enhanced photocatalytic performance. Appl Surf Sci 311:609–613. https://doi.org/10.1016/j.apsusc.2014.05.118

Jiang J, Oberdörster G, Elder A, Gelein R, Mercer P, Biswas P (2008) Does nanoparticle activity depend upon size and crystal phase? Nanotoxicology 2:33–42. https://doi.org/10.1080/17435390701882478

Jung S-H, Oh E, Lee K-H, Yang Y, Park CG, Park W, Jeong S-H (2008) Sonochemical preparation of shape-selective ZnO nanostructures. Crystal Growth & Design 8:265–269. https://doi.org/10.1021/cg070296l

Kamal T, Khan SB, Asiri AM (2016) Synthesis of zero-valent Cu nanoparticles in the chitosan coating layer on cellulose microfibers: evaluation of azo dyes catalytic reduction. Cellulose 23:1911–1923. https://doi.org/10.1007/s10570-016-0919-9

Kar A, Patra A (2014) Recent development of core-shell SnO_2 nanostructures and their potential applications. Journal of Materials Chemistry C 2:6706–6722. https://doi.org/10.1039/C4TC01030B

Kawashima N, Zhu QY, Gerson AR (2012) The selective growth of rutile thin films using radio-frequency magnetron sputtering.

Thin Solid Films 520:3884–3891. https://doi.org/10.1016/j.tsf.2012.01.021

Kennedy MK, Kruis FE, Fissan H, Mehta BR, Stappert S, Dumpich G (2002) Tailored nanoparticle films from monosized tin oxide nanocrystals: particle synthesis, film formation, and size-dependent gas-sensing properties. J Appl Phys 93:551–560. https://doi.org/10.1063/1.1525855

Kharissova OV, Dias HVR, Kharisov BI, Pérez BO, Pérez VMJ (2013) The greener synthesis of nanoparticles. Trends Biotechnol 31:240–248. https://doi.org/10.1016/j.tibtech.2013.01.003

Kim SP, Choi MY, Choi HC (2016) Photocatalytic activity of SnO_2 nanoparticles in methylene blue degradation. Mater Res Bull 74:85–89. https://doi.org/10.1016/j.materresbull.2015.10.024

Kim, J., 2014. Ti-based nanostructured materials for lithium-ion batteries

Konstantin Stanislavsky – Bella Merlin – Google Books [WWW Document], n.d. URL https://books.google.ca/books?hl=en&lr=&id=kWJgDwAAQBAJ&oi=fnd&pg=PT10&dq=Merlin+et+al.,+2018&ots=TSHIGPu9Xr&sig=UZaGaYQPcc3X8B5jEW5d–cyczoc#v=onepage&q&f=false (accessed 5.26.20).

Kostedt WL IV, Ismail AA, Mazyc DW (2008) Impact of heat treatment and composition of ZnO-TiO2 nanoparticles for photocatalytic oxidation of an azo dye. Ind Eng Chem Res 47:1483–1487. https://doi.org/10.1021/ie071255p

Krishnakumar T, Pinna N, Kumari KP, Perumal K, Jayaprakash R (2008) Microwave-assisted synthesis and characterization of tin oxide nanoparticles. Mater Lett 62:3437–3440. https://doi.org/10.1016/j.matlet.2008.02.062

Król A, Pomastowski P, Rafińska K, Railean-Plugaru V, Buszewski B (2017) Zinc oxide nanoparticles: synthesis, antiseptic activity and toxicity mechanism. Adv Coll Interface Sci 249:37–52. https://doi.org/10.1016/j.cis.2017.07.033

Lang C, Mission EG, Fuaad AA, Shaalan AM (2021) Nanoparticle tools to improve and advance precision practices in the Agri-foods Sector towards sustainability – a review. J Clean Prod 293:126063. https://doi.org/10.1016/j.jclepro.2021.126063

Latha P, Dhanabackialakshmi R, Kumar PS, Karuthapandian S (2016) Synergistic effects of trouble free and 100% recoverable CeO/Nylon nanocomposite thin film for the photocatalytic degradation of organic contaminants. Sep Purif Technol 168:124–133. https://doi.org/10.1016/j.seppur.2016.05.038

Lei B, Li B, Zhang H, Zhang L, Cong Y, Li W (2007) Synthesis and luminescence properties of cube-structured $CaSnO_3/RE^{3+}$ (RE=Pr, Tb) long-lasting phosphors. J Electrochem Soc 154:H623. https://doi.org/10.1149/1.2734775

Letia IA, Groza A (2009) Contextual extension with concept maps in the argument interchange format. Lecture Notes in Computer Science (including subseries Lecture Notes in Artificial Intelligence and Lecture Notes in Bioinformatics) 5384 LNAI, 72–89. https://doi.org/10.1007/978-3-642-00207-6_5

Li M, Zhou W-P, Marinkovic NS, Sasaki K, Adzic RR (2013) The role of rhodium and tin oxide in the platinum-based electrocatalysts for ethanol oxidation to CO_2. Electrochim Acta 104:454–461. https://doi.org/10.1016/j.electacta.2012.10.046

Liang D, Liu S, Guo Y, Wang Z, Jiang W, Liu C, Ding W, Wang H, Wang N, Zhang Z (2017) Crystalline size-control of SnO_2 nanoparticles with tunable properties prepared by HNO_3-ethanol assisted precipitation. J Alloy Compd 728:118–125. https://doi.org/10.1016/j.jallcom.2017.07.293

Liqiang J, Yichun Q, Baiqi W, Li S, Baojiang J, Libin Y, Wei F, Honggang F, Jiazhong S (2006) Review of photoluminescence performance of nano-sized semiconductor materials and its relationships with photocatalytic activity. Sol Energy Mater Sol Cells 90:1773–1787. https://doi.org/10.1016/j.solmat.2005.11.007

Liu B, Cheng CW, Chen R, Shen ZX, Fan HJ, Sun HD (2010) fine structure of ultraviolet photoluminescence of tin oxide nanowires. The Journal of Physical Chemistry C 114:3407–3410. https://doi.org/10.1021/jp9104294

Liu X, Xu D, Zhang D, Zhang G, Zhang L (2016) Superior performance of 3 D Co-Ni bimetallic oxides for catalytic degradation of organic dye: investigation on the effect of catalyst morphology and catalytic mechanism. Applied Catalysis B: Environmental 186. https://doi.org/10.1016/j.apcatb.2016.01.005

Ljubas D, Smoljanić G, Juretić H (2015) Degradation of methyl orange and congo red dyes by using TiO_2 nanoparticles activated by the solar and the solar-like radiation. J Environ Manage 161:83–91. https://doi.org/10.1016/j.jenvman.2015.06.042

Lq X, Wkh XRI, Wkh HIRU, Ri H, Ri R, Dqg F, Ri F, Dqg F (n.d) diss – Taib 2009 25

Madkour LH (2017) Ecofriendly green biosynthesized of metallic nanoparticles: bio-reduction mechanism, characterization and pharmaceutical applications in biotechnology industry. Global Drugs and Therapeutics 3:1–11. https://doi.org/10.15761/gdt.1000144

Magee JW, Zhou W-P, White MG (2014) Promotion of Pt surfaces for ethanol electro-oxidation by the addition of small SnO_2 nanoparticles: activity and mechanism. Appl Catal B 152–153:397–402. https://doi.org/10.1016/j.apcatb.2014.01.057

Majumder A, Gupta B, Gupta AK (2019) Pharmaceutically active compounds in aqueous environment: a status, toxicity and insights of remediation. Environ Res 176:108542. https://doi.org/10.1016/j.envres.2019.108542

Mascolo G, Comparelli R, Curri ML, Lovecchio G, Lopez A, Agostiano A (2007) Photocatalytic degradation of methyl red by TiO_2: comparison of the efficiency of immobilized nanoparticles versus conventional suspended catalyst. J Hazard Mater 142:130–137. https://doi.org/10.1016/j.jhazmat.2006.07.068

Matussin S, Harunsani MH, Tan AL, Khan MM (2020) Plant-extract-mediated SnO_2 nanoparticles: synthesis and applications. ACS Sustainable Chemistry & Engineering 8:3040–3054. https://doi.org/10.1021/acssuschemeng.9b06398

Meduri P, Pendyala C, Kumar V, Sumanasekera GU, Sunkara MK (2009) Hybrid tin oxide nanowires as stable and high capacity anodes for Li-ion batteries. Nano Lett 9:612–616. https://doi.org/10.1021/nl802864a

Mevada C, Chandran PS, Mukhopadhyay M (2020) Room-temperature synthesis of tin oxide nanoparticles using gallic acid monohydrate for symmetrical supercapacitor application. Journal of Energy Storage 28:101197. https://doi.org/10.1016/j.est.2020.101197

Mezzelani M, Gorbi S, Regoli F (2018) Pharmaceuticals in the aquatic environments: evidence of emerged threat and future challenges for marine organisms. Mar Environ Res 140:41–60. https://doi.org/10.1016/j.marenvres.2018.05.001

Mishra S, Zhang W, Lin Z, Pang S, Huang Y, Bhatt P, Chen S (2020) Carbofuran toxicity and its microbial degradation in contaminated environments. Chemosphere 259:127419. https://doi.org/10.1016/j.chemosphere.2020.127419

Mohammad A, Khan ME, Cho MH, Yoon T (2021) Adsorption promoted visible-light-induced photocatalytic degradation of antibiotic tetracycline by tin oxide/cerium oxide nanocomposite. Appl Surf Sci 565:150337. https://doi.org/10.1016/j.apsusc.2021.150337

Mohan L, Anandan C, Rajendran N (2015) Electrochemical behavior and effect of heat treatment on morphology, crystalline structure of self-organized TiO_2 nanotube arrays on Ti-6Al-7Nb for biomedical applications. Mater Sci Eng, C 50:394–401. https://doi.org/10.1016/j.msec.2015.02.013

Mohanta D, Ahmaruzzaman M (2021a) Facile fabrication of novel Fe_3O_4-SnO_2-gC_3N_4 ternary nanocomposites and their photocatalytic properties towards the degradation of carbofuran. Chemosphere 285:131395. https://doi.org/10.1016/j.chemosphere.2021.131395

Mohanta D, Ahmaruzzaman M (2021b) Au-SnO_2-CdS ternary nanoheterojunction composite for enhanced visible light-induced photodegradation of imidacloprid. Environ Res 201:111586. https://doi.org/10.1016/j.envres.2021.111586

Mohanta D, Ahmaruzzaman M (2021c) Novel Ag-SnO_2-βC_3N_4 ternary nanocomposite based gas sensor for enhanced low-concentration NO_2 sensing at room temperature. Sens Actuators, B Chem 326:128910. https://doi.org/10.1016/j.snb.2020.128910

Mohanta D, Raha S, Ahmaruzzaman M (2018) Biogenic green synthetic route for Janus type Ag:SnO_2 asymmetric nanocomposite arrays: plasmonic activation of wide band gap semiconductors towards photocatalytic degradation of Doripenem. Mater Lett 230:203–206. https://doi.org/10.1016/j.matlet.2018.07.079

Momeni K, Attariani H, LeSar RA (2016a) Structural transformation in monolayer materials: a 2D to 1D transformation. Phys Chem Chem Phys 18:19873–19879. https://doi.org/10.1039/C6CP04007A

Momeni S, Nasrollahzadeh M, Rustaiyan A (2016) Green synthesis of the Cu/ZnO nanoparticles mediated by Euphorbia prolifera leaf extract and investigation of their catalytic activity. Journal of Colloid and Interface Science 472. https://doi.org/10.1016/j.jcis.2016.03.042

Moreno MS, Punte G, Rigotti G, Mercader RC, Weisz AD, Blesa MA (2001) Kinetic study of the disproportionation of tin monoxide. Solid State Ionics 144:81–86. https://doi.org/10.1016/S0167-2738(01)00882-7

Muthuvinothini A, Stella S (2019) Green synthesis of metal oxide nanoparticles and their catalytic activity for the reduction of aldehydes. Process Biochem 77:48–56. https://doi.org/10.1016/j.procbio.2018.12.001

Nabi Z, Kellou A, Méçabih S, Khalfi A, Benosman N (2003) Optoelectronic properties of rutile SnO_2 and orthorhombic SnS and SnSe compounds. Mater Sci Eng, B 98:104–115. https://doi.org/10.1016/S0921-5107(02)00386-0

Nagarajan S, Arumugam Kuppusamy K (2013) Extracellular synthesis of zinc oxide nanoparticle using seaweeds of Gulf of Mannar. India Journal of Nanobiotechnology 11:39. https://doi.org/10.1186/1477-3155-11-39

Naje, A., 2003. Preparation and characterization of SnO_2 nanoparticles. International Journal of Innovative Research in Science, Engineering and Technology 2

Nilavazhagan S, Muthukumaran S, Ashokkumar M (2014) Structural, optical and morphological properties of La, Cu co-doped SnO_2 nanocrystals by co-precipitation method. Opt Mater 37:425–432. https://doi.org/10.1016/j.optmat.2014.07.003

Nipa ST, Rahman MW, Saha R, Hasan MM, Deb A (2019) Jute stick powder as a potential low-cost adsorbent to uptake methylene blue from dye enriched wastewater. Desalin Water Treat 153:279–287. https://doi.org/10.5004/dwt.2019.23767

Ong HR, Khan MMR, Ramli R, Yunus RM, Rahman MW, Hong CS, Ahmad MS (2018) Formation of CuO nanoparticle in glycerol and its catalytic activity for alkyd resin synthesis. Materials Today: Proceedings 5:3165–3175. https://doi.org/10.1016/j.matpr.2018.01.124

Otieno PO, Lalah JO, Virani M, Jondiko IO, Schramm K-W (2010) Soil and water contamination with carbofuran residues in agricultural farmlands in Kenya following the application of the technical formulation Furadan. J Environ Sci Health B 45:137–144. https://doi.org/10.1080/03601230903472058

Oviedo J, Gillan MJ (2001) First-principles study of the interaction of oxygen with the SnO_2(110) surface. Surf Sci 490:221–236. https://doi.org/10.1016/S0039-6028(01)01372-3

Oviedo J, Gillan MJ (2002) Reconstructions of strongly reduced SnO_2(110) studied by first-principles methods. Surf Sci 513:26–36. https://doi.org/10.1016/S0039-6028(02)01725-9

Park M-S, Wang G-X, Kang Y-M, Wexler D, Dou S-X, Liu H-K (2007) Preparation and electrochemical properties of SnO_2 nanowires for application in lithium–ion batteries. Angewandte Chemie International Edition 46:750–753. https://doi.org/10.1002/anie.200603309

Parwaz Khan AA, Khan A, Asiri AM (2016) Chemistry of nanoscience and technology. Nanomaterials and Nanocomposites, Wiley Online Books. https://doi.org/10.1002/9783527683772.ch2

Patel M, Kumar R, Kishor K, Mlsna T, Pittman CU, Mohan D (2019) Pharmaceuticals of emerging concern in aquatic systems: chemistry, occurrence, effects, and removal methods. Chem Rev 119:3510–3673. https://doi.org/10.1021/acs.chemrev.8b00299

Patil GE, Kajale DD, Gaikwad VB, Jain GH (2012) Preparation and characterization of SnO_2 nanoparticles by hydrothermal route. International Nano Letters 2:17. https://doi.org/10.1186/2228-5326-2-17

Prasad R, Bhattacharyya A, Nguyen QD (2017) Nanotechnology in sustainable agriculture: recent developments, challenges, and perspectives. Front Microbiol 8:1014. https://doi.org/10.3389/fmicb.2017.01014

Prieto-Rodriguez L, Miralles-Cuevas S, Oller I, Agüera A, Puma GL, Malato S (2012) Treatment of emerging contaminants in wastewater treatment plants (WWTP) effluents by solar photocatalysis using low TiO_2 concentrations. J Hazard Mater 211–212:131–137. https://doi.org/10.1016/j.jhazmat.2011.09.008

Rahman MW, Castellero A, Enzo S, Livraghi S, Giamello E, Baricco M (2011) Effect of Mg-Nb oxides addition on hydrogen sorption in MgH_2. J Alloy Compd 509:S438–S443. https://doi.org/10.1016/j.jallcom.2011.02.064

Safavi A, Momeni S (2012) Highly efficient degradation of azo dyes by palladium/hydroxyapatite/Fe_3O_4 nanocatalyst. J Hazard Mater 201–202:125–131. https://doi.org/10.1016/j.jhazmat.2011.11.048

Sangami G, Dharmaraj N (2012) UV-visible spectroscopic estimation of photodegradation of rhodamine-B dye using tin(IV) oxide nanoparticles. Spectrochim Acta Part A Mol Biomol Spectrosc 97:847–852. https://doi.org/10.1016/j.saa.2012.07.068

Santhi K, Rani C, Karuppuchamy S (2016) Synthesis and characterization of a novel SnO/SnO_2 hybrid photocatalyst. J Alloy Compd 662:102–107. https://doi.org/10.1016/j.jallcom.2015.12.007

Sarkar S, Das R, Choi H, Bhattacharjee C (2014) Involvement of process parameters and various modes of application of TiO_2 nanoparticles in heterogeneous photocatalysis of pharmaceutical wastes – a short review. RSC Adv 4:57250–57266. https://doi.org/10.1039/C4RA09582K

Savolainen K, Backman U, Brouwer D, Fadeel B, Fernandes T, Kuhlbusch T, Landsiedel R, Lynch I, Pylkkanen L (2013) Nanosafety in Europe 2015–2025: towards safe and sustainable nanomaterials and nanotechnology innovations, Finnish Institute of Occupational Health

Scott NR (2005) Nanotechnology and animal health. Revue scientifique et technique (International Office of Epizootics) 24, 425–432. https://doi.org/10.20506/rst.24.1.1579

Seabra AB, Durán N (2015) Nanotoxicology of Metal Oxide Nanoparticles Metals 5:934–975. https://doi.org/10.3390/met5020934

Serpone N, Artemev YM, Ryabchuk VK, Emeline AV, Horikoshi S (2017) Light-driven advanced oxidation processes in the disposal of emerging pharmaceutical contaminants in aqueous media: A brief review. Current Opinion in Green and Sustainable Chemistry 6:18–33. https://doi.org/10.1016/j.cogsc.2017.05.003

Shahverdi A–R, Shakibaie M, Nazari P (2011) Basic and Practical procedures for microbial synthesis of nanoparticles BT – metal nanoparticles in microbiology, in: Rai, M., Duran, N. (Eds.), . Springer Berlin Heidelberg, Berlin, Heidelberg, pp. 177–195. https://doi.org/10.1007/978-3-642-18312-6_8

Shaikh FI, Chikhale LP, Mulla IS, Suryavanshi SS (2018) Facile co-precipitation synthesis and ethanol sensing performance of Pd loaded Sr doped SnO_2 nanoparticles. Powder Technol 326:479–487. https://doi.org/10.1016/j.powtec.2017.12.028

Shukla S, Chaudhary S, Umar A, Chaudhary GR, Kansal SK, Mehta SK (2016) Surfactant functionalized tungsten oxide nanoparticles with enhanced photocatalytic activity. Chem Eng J 288:423–431. https://doi.org/10.1016/j.cej.2015.12.039

Singh V, lehri alok, Singh N (2018) Singh et al–2018–International Journal of Environmental Science and Technology

Sk M, Yue C (2014) Synthesis of polyaniline nanotubes using the self–assembly behavior of vitamin C: A mechanistic study and application in electrochemical supercapacitors. Journal of Materials Chemistry A 2:2830. https://doi.org/10.1039/c3ta14309k

Song KC, Kang Y (2000) Preparation of high surface area tin oxide powders by a homogeneous precipitation method. Mater Lett 42:283–289. https://doi.org/10.1016/S0167-577X(99)00199-8

Stanulis A, Sakirzanovas S, Van Bael M, Kareiva A (2012) Sol-gel (combustion) synthesis and characterization of different alkaline earth metal (Ca, Sr, Ba) stannates. J Sol-Gel Sci Technol 64:643–652. https://doi.org/10.1007/s10971-012-2896-2

Subair R, Tripathi BP, Formanek P, Simon F, Uhlmann P, Stamm M (2016) Polydopamine modified membranes with in situ synthesized gold nanoparticles for catalytic and environmental applications. Chem Eng J 295:358–369. https://doi.org/10.1016/j.cej.2016.02.105

Suthakaran S, Dhanapandian S, Krishnakumar N, Ponpandian N, Dhamodharan P, Anandan M (2020) Surfactant-assisted hydrothermal synthesis of Zr doped SnO_2 nanoparticles with photocatalytic and supercapacitor applications. Mater Sci Semicond Process 111:104982. https://doi.org/10.1016/j.mssp.2020.104982

Suttiponparnit K, Jiang J, Sahu M, Suvachittanont S, Charinpanitkul T, Biswas P (2010) Role of surface area, primary particle size, and crystal phase on titanium dioxide nanoparticle dispersion properties. Nanoscale Res Lett 6:27. https://doi.org/10.1007/s11671-010-9772-1

Tammina SK, Mandal BK (2016) Tyrosine mediated synthesis of SnO_2 nanoparticles and their photocatalytic activity towards Violet 4 BSN dye. J Mol Liq 221:415–421. https://doi.org/10.1016/j.molliq.2016.05.079

Tammina SK, Mandal BK, Kadiyala NK (2018) Photocatalytic degradation of methylene blue dye by nonconventional synthesized SnO_2 nanoparticles. Environmental Nanotechnology, Monitoring and Management 10:339–350. https://doi.org/10.1016/j.enmm.2018.07.006

Thakkar KN, Mhatre SS, Parikh RY (2010) Biological synthesis of metallic nanoparticles. Nanomedicine: Nanotechnology. Biology and Medicine 6:257–262. https://doi.org/10.1016/j.nano.2009.07.002

Thamarai Selvi E, Meenakshi Sundar S (2018) Popcorn like morphology and absence of room temperature ferromagnetism in Ni doped SnO_2 nanoparticles. J Mater Sci: Mater Electron 29:38–48. https://doi.org/10.1007/s10854-017-7885-3

Tin: its oxidation states and reactions with it – MEL Chemistry [WWW Document], n.d. URL https://melscience.com/US–en/articles/tin–its–oxidation–states–and–reactions–it/ (accessed 5.26.20)

Tišler T, Jemec A, Mozetič B, Trebše P (2009) Hazard identification of imidacloprid to aquatic environment. Chemosphere 76:907–914. https://doi.org/10.1016/j.chemosphere.2009.05.002

Tiwari JN, Tiwari RN, Kim KS (2012) Zero-dimensional, one-dimensional, two-dimensional and three-dimensional nanostructured materials for advanced electrochemical energy devices. Prog Mater Sci 57:724–803. https://doi.org/10.1016/j.pmatsci.2011.08.003

Van Benschoten JE, Reed BE, Matsumoto MR, McGarvey PJ (1994) Metal removal by soil washing for an iron oxide coated sandy soil. Water Environ Res 66:168–174. https://doi.org/10.2175/wer.66.2.11

Varma KS, Tayade RJ, Shah KJ, Joshi PA, Shukla AD, Gandhi VG (2020) Photocatalytic degradation of pharmaceutical and pesticide compounds (PPCs) using doped TiO_2 nanomaterials: A review. Water-Energy Nexus 3:46–61. https://doi.org/10.1016/j.wen.2020.03.008

Vatanparast M, Taghizadeh MT (2016) One–step hydrothermal synthesis of tin dioxide nanoparticles and its photocatalytic degradation of methylene blue. J Mater Sci: Mater Electron 27:54–63. https://doi.org/10.1007/s10854-015-3716-6

Veerabhadrayya M, Ananda Kumari R, Nagabhushana H, Basavaraj RB (2018) Structural and optical properties of Mg^{2+} doped tin oxide nanoparticles prepared via green combustion synthesis. Materials Today: Proceedings 5:21147–21155. https://doi.org/10.1016/j.matpr.2018.06.513

Velempini T, Prabakaran E, Pillay K (2021) Recent developments in the use of metal oxides for photocatalytic degradation of pharmaceutical pollutants in water—a review. Materials Today Chemistry 19:100380. https://doi.org/10.1016/j.mtchem.2020.100380

Vijukumar VG, Prem AA (2018) Green synthesis and characterization of iron oxide nanoparticles using Phyllanthus niruri extract. Oriental Journal of Chemistry 34:2583–2589. https://doi.org/10.13005/ojc/340547

Wang B, Zhu LF, Yang YH, Xu NS, Yang GW (2008) Fabrication of a SnO_2 nanowire gas sensor and sensor performance for hydrogen. The Journal of Physical Chemistry C 112:6643–6647. https://doi.org/10.1021/jp8003147

Wang C, Zhou Y, Ge M, Xu X, Zhang Z, Jiang JZ (2010a) Large-scale synthesis of SnO_2 nanosheets with high lithium storage capacity. J Am Chem Soc 132:46–47. https://doi.org/10.1021/ja909321d

Wang H, Sun F, Zhang Y, Li L, Chen H, Wu Q, Yu JC (2010b) Photochemical growth of nanoporous SnO_2 at the air–water interface and its high photocatalytic activity. J Mater Chem 20:5641–5645. https://doi.org/10.1039/B926930D

Wang J, Xu Y, Xu W, Zhang M, Chen X (2015) Simplified preparation of SnO_2 inverse opal for methanol gas sensing performance. Microporous Mesoporous Mater 208:93–97. https://doi.org/10.1016/j.micromeso.2015.01.038

Wiberg N (2002) Holleman–Wiberg's inorganic chemistry. J Chem Educ 79:944. https://doi.org/10.1021/ed079p944

Wu S, Cao H, Yin S, Liu X, Zhang X (2009) Amino acid-assisted hydrothermal synthesis and photocatalysis of SnO_2 nanocrystals. The Journal of Physical Chemistry C 113:17893–17898. https://doi.org/10.1021/jp9068762

Wu HB, Chen JS, Lou (David) XW, Hng HH (2011) Synthesis of SnO_2 hierarchical structures assembled from nanosheets and their lithium storage properties. The Journal of Physical Chemistry C 115:24605–24610. https://doi.org/10.1021/jp208158m

Xi G, Ye J (2010) Ultrathin SnO_2 nanorods: template- and surfactant-free solution phase synthesis, growth mechanism, optical, gas-sensing, and surface adsorption properties. Inorg Chem 49:2302–2309. https://doi.org/10.1021/ic902131a

Xiong J, Wang Y, Xue Q, Wu X (2011) Synthesis of highly stable dispersions of nanosized copper particles using L-ascorbic acid. Green Chem 13:900–904. https://doi.org/10.1039/C0GC00772B

Yang J, Li X, Lang J, Yang L, Wei M, Gao M, Liu X, Zhai H, Wang R, Liu Y, Cao J (2011) Synthesis and optical properties of Eu-doped ZnO nanosheets by hydrothermal method. Mater Sci Semicond Process 14:247–252. https://doi.org/10.1016/j.mssp.2011.04.002

Zamand N, Nakhaei Pour A, Housaindokht MR, Izadyar M (2014) Size-controlled synthesis of SnO_2 nanoparticles using reverse microemulsion method. Solid State Sci 33:6–11. https://doi.org/10.1016/j.solidstatesciences.2014.04.005

Zeng H, Xu X, Bando Y, Gautam UK, Zhai T, Fang X, Liu B, Golberg D (2009) Template deformation-tailored ZnO nanorod/nanowire

arrays: full growth control and optimization of field-emission. Adv Func Mater 19:3165–3172. https://doi.org/10.1002/adfm.200900714

Zhang G, Liu M (1999) Preparation of nanostructured tin oxide using a sol-gel process based on tin tetrachloride and ethylene glycol. J Mater Sci 34:3213–3219. https://doi.org/10.1023/A:1004685907751

Zhang L, Lv F, Zhang W, Li R, Zhong H, Zhao Y, Zhang Y, Wang X (2009a) Photo degradation of methyl orange by attapulgite-SnO_2-TiO_2 nanocomposites. J Hazard Mater 171:294–300. https://doi.org/10.1016/j.jhazmat.2009.05.140

Zhang R, Chen L, Ren Y, Wang J (2009b) Brewing MnWO4 microspheres on the eggshell membrane at room temperature. Russ J Inorg Chem 54:1189–1192. https://doi.org/10.1134/S003602360908004X

Zhang C, wang P, Li F (2011) First-principles study on surface magnetism in co-doped (110) SnO_2 thin film. Solid State Sciences 13:1608–1611. https://doi.org/10.1016/j.solidstatesciences.2011.06.010

Zhang K, Liu YD, Choi HJ (2012) Carbon nanotube coated snowman-like particles and their electro-responsive characteristics. Chem Commun 48:136–138. https://doi.org/10.1039/C1CC16140G

Zhong L-S, Hu J-S, Liang H-P, Cao A-M, Song W-G, Wan L-J (2006) Self-assembled 3D flowerlike iron oxide nanostructures and their application in water treatment. Advanced Materials 18:2426–2431. https://doi.org/10.1002/adma.200600504

Zikalala N, Matshetshe K, Parani S, Oluwafemi OS (2018) Biosynthesis protocols for colloidal metal oxide nanoparticles. Nano-Structures & Nano-Objects 16:288–299. https://doi.org/10.1016/j.nanoso.2018.07.010